Cryo-adapted bacterial copiotrophs from a Trans-Himalayan lake-desert ecosystem as biogeothermometers of warming, mitigators of perturbation, and candidates for biodegradation

Sumit Chatterjee[1], Subhajit Dutta[1], Jit Ghosh[1], Swapneel Saha[1], Mahamadul Mondal[1], Jagannath Sarkar[1,$], Nibendu Mondal[1,#], and Wriddhiman Ghosh[1,*]

Author Address:
[1] Department of Biological Sciences, Bose Institute, Kolkata, India

Present Address:
[$] Faculty of Engineering and Natural Sciences, Tampere University, Finland
[#] Department of Microbiology and Cell Science, Fort Lauderdale Research and Education Center, University of Florida, USA

Correspondence:
***** Wriddhiman Ghosh (wriman@jcbose.ac.in, wriman@rediffmail.com)

Keywords: Trans-Himalayan deserts and lakes, psychrophilic and cryo-adapted bacteria, climate warming, antibiosis, microbiome protection, organic matter degradation

Running title: Ecological essentials of cryo-adapted copiotrophs

---

ABSTRACT

A Trans-Himalayan lake-desert ecosystem was explored for the low-to-high temperature adaptations of native copiotrophic psychrophiles that have the potentials for rendering substantive carbon remineralization under natural and/or anthropogenically influenced conditions of high organic matter delivery to the environment. Overall 27 species, classified across 15 genera of Actinomycetota, Bacillota, Bacteroidota, and Pseudomonadota, were isolated from the brackish-water and sediment-surface of Tso Moriri (a massive lacustrine body on the Changthang plateau that remains frozen for approximately one third of the year), and the fine talus covering a lake-side rocky mountain. In Luria broth, all the isolates grew at 4°C and 15°C; 13 of them grew, while 14 retained 19-99% cells in metabolically-active state, at -10°C; 23, 11, and none grew at 28°C, 37°C, and 42°C respectively. A *Cryobacterium* was most heat-susceptible, whereas some -10°C-growing *Arthrobacter*, *Microbacterium*, *Paenarthrobacter*, *Pseudomonas* and *Streptomyces* were most warming-resilient, among the present isolates. Catabolizing different simple/complex organic compounds, all isolates accomplished low/moderate/high growths at 4°C; 20 performed low growths at -10°C. Taxonomy/phylogeny did

not determine the isolates' growth/survival across the temperature-range tested. Lake-water and rock-dust isolates had the widest, while lake-sediment-dwellers had the narrowest, temperature-window for growth/survival. Rock-dust and lake-water isolates had more genes for low and high temperature adaptations, compared to the lake-sediment isolates. In co-cultures, most actinobacterial isolates inhibited the growth of mesophilic bacteria from warmer ecosystems, plus non-actinobacteria and actinobacteria from native/adjoining habitats. The data hold implications for biodegradation in cold/frigid territories, negative feedback control/reversal of warming, and microbiome protection from infiltration amidst climate change.

IMPORTANCE

Phylogenetically diverse, cold-adapted copiotrophic bacteria were retrieved from a Trans-Himalayan lake-desert ecosystem, and tested for chemoorganoheterotrophic growth at temperatures between -10°C and 42°C. Albeit growth dwindled at ≥28°C, most of the isolates thrived on simple as well as complex organic substances under freezing condition, which makes them prospective constituents of biodegradation reactors suitable for high-altitude/latitude deployment. In the natural habitats of the psychrophilic isolates, cessation of organotrophic activities at elevated temperatures would stop simple fatty acids and CO_2 production, which in turn would preempt methanogenesis, undo greenhouse effect, and reverse environmental thawing (usher cooling). Such negative feedback control of homeostasis is fraught with the danger of microbiome takeover by thermally-better-adapted foreign organisms. Consequently, ecosystem preservation rests on the native microflora's ability to resist external invasion. At 28°C, majority of the actinobacterial isolates inhibited bacteria from discrete higher-temperature ecosystems; they can, therefore, be viewed as the defenders of the cold/frigid ecosystem.

INTRODUCTION

Microbial life at low temperatures is constrained by a number of biophysical and biochemical adversities (1, 2). However, across the seasonally or perpetually frozen alpine/polar territories of the Earth's biosphere, barren soils, outwardly life-less rocky terrains, and most conspicuously, numerous limnic and fluvioglacial features, harbor considerably diversified microbiomes (3, 4) that in turn sustain highly climate-sensitive ecosystems via biogeochemical cycling of carbon and other elements (5–7).

Throughout the high-latitude and high-altitude areas of the globe, copious endolithic and chasmolithic microbial communities colonize the rocky terrains and contribute actively or

passively to the weathering of rocks into dust and scree, thereby promoting sediment and soil formation (8, 9). Supraglacial and subglacial microbiomes drive considerable biogeochemical activities (10–12). The former types accelerate the melting of glaciers (13, 14), while post deglaciation the latter types release profuse greenhouse gases, such as carbon dioxide (CO_2) and methane (CH_4), into the atmosphere (15–17). Microbiomes thriving in young as well as matured soils, including those associated with permafrosts, and biocrusts covering deglaciated moraines and rock surfaces, render temporally slow but spatially extensive, fixation and remineralization of carbon (18, 19). Furthermore, approximately, 25 million lacustrine bodies (20), together with the vast expanses of thermokarst landforms, sequester huge amount of organic carbon by remaining frozen for a substantial part of the year, and emit enormous volumes of CO_2 and CH_4 upon thawing (21–25).

In all temporarily or permanently frozen ecosystems, microbial activities and proliferation apparently remain subdued as long as the temperature remains below or around 0°C (19, 26). However, organotrophic growth, and thereby remineralization of carbon and emission of greenhouse gases, starts once the temperature rises and cryoturbation takes place on a seasonal or climatic scale (19, 27–31). Greenhouse effect, at any spatiotemporal level, is thought to enhance microbial activities and growth, which in turn induces further thawing of the environment (19, 32). Such positive feedback cycles (27, 32, 33) can, in the long run, alter the structures and functions of microbiomes, and thereby entire ecosystems, within the cold/frigid realm.

To understand the functioning of cold/frigid ecosystems, and in order to manage them in a sustainable way, we require comprehensive information on the scopes of carbon cycling and sequestration around the freezing point of water. For that purpose, chemoorganoheterotrophic capabilities of autochthonous microorganisms need to be delineated at near-zero and sub-zero degree Celsius, via extensive pure-culture-based investigations. Furthermore, in the context of global warming in the present era, it is imperative to appreciate the homeostatic vulnerabilities of alpine/polar microbiomes alongside their potential intrinsic resilience against perturbations. This would subsequently help mitigate impending microbiome (and habitat) alterations triggered by climate change across the global cryosphere. Towards that end, we require comprehensive data on how psychrophilic microorganisms (34–36) respond to different levels of warming in terms of population-level growth or survival. Concurrently, in relation to plausible microbiome transformation within cold/frigid ecosystems due to global warming, we need to know whether cold-adapted microbial communities have any indigenous safeguard against infiltration of organisms from warmer territories (37, 38).

The present study of pure-culture microbiology explored three adjacent environments (habitats) within a Trans-Himalayan lake-desert ecosystem, centered on the massive fresh-to-brackish water body called Tso Moriri (vernacular meaning: lake amid the mountains), which is situated on the cold arid Changthang plateau of eastern Ladakh, India (Figs. 1a-c). Phylogenetically diverse chemoorganoheterotrophic bacterial psychrophiles were isolated and characterized from Tso Moriri's sediment, and water that remains frozen for approximately one third of the year. Psychrophilic heterotrophs were also isolated from the weathered rock dust (fine talus and scree particles) that covers the hill overlooking the western bank of the lake (Figs. 1d-g). Prior to the isolation of pure cultures, the water, sediment and talus samples were subjected to iterative cycles of freezing and thawing. This ensured that the bacterial strains retrieved were cryo-adapted (capable of rendering growth, whether little or substantial, at -10°C), or at least cryo-tolerant (adept in population-level survival, i.e. retention of >1% cells in metabolically-active state, at -10°C), in nature.

A separate time-series investigation of biogeochemistry, carried out by our laboratory (Chatterjee et al., unpublished) at the same sample sites explored in this study, had shown that after the summer months (just before the winter), concentration of total carbon in the surficial lake-water reached 80 mg L^{-1}, while total carbon content of the surficial samples of lake-sediment and weathered rock dust reached approximately 2% (w/w) and 1% (w/w) respectively. In view of these findings [notably, the aforesaid numbers are reasonably close to the carbon content values reported from many tropical marine ecosystems (39, 40)], the present enrichment and isolation strategy specifically targeted cryo-adapted, or cryo-tolerant, copiotrophs that possess the potentials for rendering substantive carbon remineralization under cold and frigid conditions. The overall objective was to ensure that the organotrophic growth potentials exhibited by the new isolates *in vitro* held direct implications for the scope of *in situ* organic matter degradation across alpine/polar ecosystems experiencing high carbon delivery to the environment, naturally and/or under anthropogenic influence.

In the aforesaid context, it was first investigated whether the copiotrophic psychrophiles isolated in nutrient-rich medium could grow by catabolizing different simple or complex organic substrates at near-zero and sub-zero degree Celsius. Experiments were then conducted to know how the growth and activity of the isolates were affected by different levels of warming. The data obtained *in vitro* were evaluated theoretically to explore whether natural populations of the isolated bacteria could act as "biogeothermometers" chronicling *in situ* temperatures over time and space. From the contemporary perspective of heightened thawing of the cold/frigid realm, we examined whether the bacteria retrieved from the Tso Moriri area (TMA) had any aptitude for

resisting incursion of foreign microorganisms from warmer climatic territories. For this purpose we tested the antibiosis potentials of the current isolates against higher-temperature-adapted bacteria retrieved previously from discrete warmer ecosystems. All phenotypic features delineated for the new isolates were appraised in the light of the organisms' genome contents. The whole repertoire of data available was eventually interpreted in the context of climate change to envisage if the indigenous psychrophiles had any role in the abatement of environmental warming. Cold/frigid ecosystems, in the present era, being exceedingly perturbed by anthropogenic waste deposition (41) possibilities were weighed for using the copiotrophic TMA psychrophiles in bioreactors designed to degrade organic litters at near-zero and sub-zero degree Celsius.

RESULTS

Cold-adapted copiotrophs from Tso Moriri lake-desert ecosystem

A sum total of 61 aerobic, copiotrophic, and freeze-thaw resilient bacterial pure-cultures, apparently dissimilar with regard to colony morphology, were enriched and isolated in Luria broth (LB), from the lake-water (Fig. 1f), lake-sediment (Fig. 1g), and rock-dust (Fig. 1e) samples. 22 of these were obtained from the weathered rock dust of the lake-side hill, while five and 34 were from the lake's water and sediment respectively (Table 1). 16S rRNA gene sequence similarities clustered the 61 isolates into 27 species-level entities that in turn were ascribable to 15 genera distributed over the phyla Actinomycetota, Bacillota, Bacteroidota and Pseudomonadota. One representative strain from each species-level cluster was selected for further characterization (Table 1).

Cold adaptations of the TMA isolates

In LB medium, all the 27 species retrieved from the Tso Moriri area could grow at 4°C (Figs. 2c-d) and 15°C (Figs. 2e-f), whereas only 13 could grow at -10°C (Figs. 2a-b). In terms of what percentage of the starting CFU density (colony-forming units mL^{-1}) remained in the culture after the stipulated period of incubation (Tables S1-S3), the extents of growth recorded at -10°C were far lower than those recorded at 4°C and 15°C. After 14 days at 4°C, the cultures of *Flavobacterium* TS_SC_2 and *Arthrobacter* TRD_SC_3 showed the lowest and highest increases in CFU density respectively. After two days at 15°C, lowest and highest increases in CFU density were exhibited by the cultures of *Flavobacterium* TS_SC_2 and *Arthrobacter* TRD_SC_8

respectively. After 28 days at -10°C, *Pseudarthrobacter* TRD_SC_9 and *Arthrobacter* TRD_SC_6 had the lowest and highest increases in CFU density respectively.

Notably, the 14 species, which could not grow in LB at -10°C, managed to maintain considerable proportions of their cell populations in divisible (Figs. 2a-b) and/or metabolically-active (Figs. 2g and S1) states, as evidenced by CFU density data, and fluorescein diacetate (FDA) staining followed by flow cytometry, respectively. After 28 days at this temperature, *Acinetobacter* TW_SC_4 and *Aeromonas* TS_SC_11 retained the lowest and highest proportions (2% and 75%) of the initial CFU density respectively, while *Pseudarthrobacter* TS_SC_4 had the lowest (19%), and *Cryobacterium* TS_SC_7 and *Sanguibacter* TS_SC_8 had the highest (99%), proportions of cell stained with FDA. Furthermore, for every bacterium lacking growth at -10°C, the percentage of metabolically-active cells exceeded the percentage of cells retaining their divisibility after 28 days of incubation, even though no significant correlation existed between the proportions of divisible and metabolically-active cells (Fig. S2a).

Growth on different simple/complex carbon compounds at zero and sub-zero degree Celsius

After 14 days of incubation at 4°C, all the bacterial species isolated from the TMA rendered at least a little growth by utilizing no less than three out of the 10, simple or complex, organic compounds tested as single chemoorganoheterotrophic substrates (Tables S4-S13). The extent of growth differed across the isolates in terms of the percentage increase in CFU density that was attributable to the utilization of the carbon compound in question (Fig. 3a; Table S14). 10 TMA isolates were found to accomplish low, moderate, or high growth on all the 10 compounds tested; these were *Aeromonas* TS_SC_11, *Arthrobacter* TRD_SC_3, *Cryobacterium* TS_SC_7, *Flavobacterium* TS_SC_2, *Flavobacterium* TS_SC_5, *Microbacterium* TRD_SC_10, *Sanguibacter* TS_SC_8, *Pseudomonas* TS_SC_12, *Pseudomonas* TS_SC_13 and *Psychrobacter* TS_SC_6. Although unable to use acetate, *Streptomyces* TRD_SC_5 could accomplish high growth on maximum number of complex carbon compounds, namely cellulose, chitin, pectin, starch and xylan; this organism also rendered moderate growth on agar, albumin and hexadecane, while its growth on benzoate was low. In contrast, *Pseudomonas* TS_SC_3, which could only render moderate growth on cellulose, and low growth on albumin and starch, was the least efficient TMA isolate in terms of chemoorganoheterotrophic utilization of the carbon substrates tested.

After 28 days of incubation at -10°C, a sum total of 20 TMA isolates were found to render low but definite growth on at least one of the 10 carbon compounds tested (Tables S15-S24),

even though in LB medium, only 13 species had exhibited low to high growth at -10°C (Figs. 2a-b; Table S1). Of the 14 TMA isolates that had failed to render -10°C-growth in LB, seven – namely, *Aeromonas* TS_SC_11 (benzoate and cellulose), *Ancylobacter* TW_SC_1 (agar and chitin), *Cryobacterium* TS_SC_7 (acetate, albumin, cellulose and pectin), *Flavobacterium* TS_SC_5 (agar), *Microbacterium* TRD_SC_10 (agar, albumin, benzoate, chitin and starch), *Pseudarthrobacter* TS_SC_4 (agar and starch), and *Pseudomonas* TS_SC_10 (agar) – could render a low level of growth attributable to the use of at least one carbon compound (Fig. 3b; Table S25). Overall, *Arthrobacter* TRD_SC_3 accomplished low levels of growth on all the 10 compounds tested, while *Streptomyces* TRD_SC_5 rendered low levels of growth on all the substrates except acetate, and *Mycetocola* TRD_SC_2 could do the same on all the carbon compounds except acetate, albumin and benzoate. Of the remaining 24 isolates, 17 could achieve low levels of growth on only a few, or just one, of the 10 organic substrates tested; seven isolates could grow on none of them (Fig. 3b; Table S25).

Extreme oligotrophy at zero and sub-zero degree Celsius

In the above experiments, growth of an isolate on a given organic substrate was defined exclusively by a positive remainder value obtained after subtracting the percentage increase in CFU density recorded for the isolate in MS solution from the percentage increase in CFU density recorded in MS plus the substrate in question (furthermore, for the two percentage terms in question, only positive values were taken into consideration). In that context, a separate scrutiny of the increases in the CFU densities of the different isolates recorded after incubation in MS solution at 4°C and -10°C revealed their extreme oligotrophic potentials.

At 4°C, after 14 days of incubation in MS solution (Table S26), CFU densities of *Microbacterium* TW_SC_2, and *Pseudomonas* strains TS_SC_1 and TS_SC_10, increased by >200% of the initial levels, whereas those of *Acinetobacter* TW_SC_4, *Arthrobacter* TRD_SC_1 and TRD_SC_6, *Microbacterium* TW_SC_3, *Mycetocola* TRD_SC_2, *Paenarthrobacter* TRD_SC_7 and *Trichococcus* TS_SC_9 increased by 6-72%. Under these conditions, CFU densities of *Arthrobacter* TRD_SC_3, *Microbacterium* TRD_SC_10, and *Streptomyces* TRD_SC_5 remained unchanged, while those of the remaining 14 strains decreased by 3-90% of the initial levels.

At -10°C, after 28 days in MS (Table S27), CFU densities of *Arthrobacter* strains TRD_SC_1 and TRD_SC_6, *Microbacterium* strains TW_SC_2 and TW_SC_3, *Mycetocola* TRD_SC_2, and *Paenarthrobacter* TRD_SC_7 increased by 10-50%, whereas those of the remaining species decreased by 2-98%, of the corresponding initial levels.

Progressive thermal susceptibility of the TMA isolates

In LB medium, 23 out of the 27 TMA isolates studied could grow at 28°C (Figs. 4a-b; Table S28), whereas only 11 could grow at 37°C (Figs. 4c-d; Table S29), and none at 42°C (Figs. 4e-f; Table S30). In terms of what percentage of the starting CFU density remained in the culture after the stipulated period of incubation, extents of growth recorded at 28°C were much higher than those recorded at 37°C.

Of the four species incapable of growing in LB at 28°C, three did not retain any CFU, while only *Arthrobacter* TRD_SC_4 retained 28% of the initial CFU density, after four days of incubation at this temperature. At the same time, three of these four isolates had 18-58% cells in metabolically-active conditions, while *Cryobacterium* TS_SC_7 had 0.2% cells in active condition (Figs. 4g and S3a).

At 37°C, 16 TMA isolates failed to grow in LB. Nine of them had zero or near-zero CFU density, while the other seven had 1-48% of the initial CFU densities, remaining in the cultures after two days of incubation. At the same time, 15 out of these 16 isolates had 4-76% cells in metabolically-active conditions, while *Cryobacterium* TS_SC_7 had 0.1% cells in active condition (Figs. 4h and S3b).

None of the 27 species retrieved from the Tso Moriri area could grow in LB at 42°C. 22 of them had zero or near-zero CFU density, while the remaining five had 1-33% of the initial CFU densities, present in the cultures after one day of incubation. At the same time, 19 out of the 27 isolates had 1-87.3% cells in metabolically-active conditions, while eight had <1% cell in active condition (Figs. 4i and S4).

Overall, the trends of LB-based population-level survival of the isolates lacking growth at ≥28°C showed that the percentage of cells remaining metabolically active at a given high temperature exceeded the percentage of cells which retained their divisibility at that temperature (Figs. 4g-i). Furthermore, for all strains susceptible to high temperatures, proportions of divisible, and metabolically active, cells remaining in the cultures after stipulated periods of incubation decreased with increase in temperature. That said, no significant correlation existed between the proportions of divisible and metabolically-active cells, across the species incapable of growth at high temperatures (Figs. S2b-d).

Differential temperature windows for growth and survival of cell populations

At every incubation temperature tested for growth in LB medium (-10°C, 4°C, 15°C, 28°C, 37°C, or 42°C), different TMA isolates exhibited different rates of increase or decrease in CFU density (Tables S31-36 show the data for the six individual temperatures). On the flip side, temperature

windows for growth (increase in CFU density) and population-level survival (retention of >1% cells in metabolically-active state), over the tested range, varied across the isolates (Fig. 5). *Arthrobacter* TRD_SC_3 and TRD_SC_8, *Microbacterium* TW_SC_2 and TW_SC_3, *Paenarthrobacter* TRD_SC_7, and Streptomyces TRD_SC_5, shared the widest temperature range over which growth was recorded (-10°C to 37°C), whereas *Flavobacterium* TS_SC_5 and *Cryobacterium* TS_SC_7 had the narrowest growth window (4°C to 15°C).

For all those 4°C-growing isolates whose growth in LB ceased at -10°C, more than 1% cells remained metabolically active at this freezing temperature (Fig. 2g); the -10°C-growing isolates, on the other hand, were likely to remain metabolically active at even lower temperatures. At ≥28°C, all the TMA isolates, except *Arthrobacter* TRD_SC_6 and *Cryobacterium* TS_SC_7, exhibited population-level survival at temperatures above the points where their growth was last recorded (Figs. 5 and 6a). For TRD_SC_6 and TS_SC_7, growth in LB was last recorded at 37°C and 15°C respectively, but their proportions of metabolically-active cells in the culture dropped below the 1% threshold at the immediately higher temperature points tested, i.e. at 42°C and 28°C respectively (Figs. 2 and 4).

So far as the most suitable temperature for LB-dependent growth was concerned (Fig. 5), 22 TMA isolates had their highest rates of increase in CFU density at 15°C. For all these isolates, except *Microbacterium* TRD_SC_10, 15°C growth rates exceeded their 4°C growth rates by orders of 10. Furthermore, for one half of the 22 TMA isolates having growth maxima at 15°C - i.e. for three *Arthrobacter* species, the two *Flavobacterium* species, and one species each of *Cryobacterium*, *Microbacterium*, *Pseudarthrobacter*, *Pseudomonas*, *Sanguibacter* and *Trichococcus* - 4°C growth rates were higher than their 28°C growth rates. In contrast, for the other half of these 22 isolates - i.e. for two *Arthrobacter* species, four *Pseudomonas* species, and one species each of *Aeromonas*, *Microbacterium*, *Paenarthrobacter*, *Pseudarthrobacter* and *Psychrobacter* - 28°C growth rates were higher than their 4°C growth rates. For *Acinetobacter* TW_SC_4, *Ancylobacter* TW_SC_1, *Microbacterium* TW_SC_2 and *Streptomyces* TRD_SC_5, maximum growth rates were recorded at 28°C. While the 15°C growth rates of all these four species were higher than their 4°C growth rates, for *Microbacterium* TW_SC_2 and *Streptomyces* TRD_SC_5 their 4°C growth rates were higher than the 37°C growth rates, but for *Acinetobacter* TW_SC_4 and *Ancylobacter* TW_SC_1 their 37°C growth rates were higher than the 4°C growth rates. For *Mycetocola* TRD_SC_2 alone, growth rate was highest at 4°C, then decreased through 28°C, and became negative at 37°C.

Antibiosis by TMA actinobacteria

Of the 15 actinobacterial species isolated from the Tso Moriri area, 11 had the ability to inhibit the growth of at least one of the six higher-temperature-adapted foreign bacteria against which antibiosis was tested, namely the Gram negative organisms *Escherichia coli* K-12, *Advenella kashmirensis* WT001, *Paracoccus* sp. SMMA_5, and the Gram positive *Bacillus subtilis* SC_1, *Bacillus licheniformis* PAMA2_SD1, and *Lysinibacillus fusiformis* LAPE1_SD1 (Fig. 7). Only the four *Arthrobacter* species represented by the strains TRD_SC_1, TRD_SC_3, TRD_SC_4 and TRD_SC_8 had no antagonistic activity against any of the six target organisms. In contrast, *Pseudarthrobacter* TRD_SC_9 and *Streptomyces* TRD_SC_5 disallowed the growth of all the six foreign bacteria targeted, while *Paenarthrobacter* TRD_SC_7 inhibited all but *Advenella kashmirensis* WT001, and *Arthrobacter* TRD_SC_6 deterred only *Lysinibacillus fusiformis* LAPE1_SD1. On the flip side of the above data, most number of TMA actinobacteria were active against *Lysinibacillus fusiformis* LAPE1_SD1, *Bacillus licheniformis* PAMA2_SD1, and *Escherichia coli* K-12, which in turn were inhibited by 11, nine and seven actinobacteria respectively. Five, four, and three TMA actinobacteria were found to inhibit the growth of *Bacillus subtilis* SC_1, *Advenella kashmirensis* WT001, and *Paracoccus* SMMA_5, respectively. Notably, none of the 12 non-actinobacterial species isolated from TMA had the ability to inhibit the growth of any of the foreign bacteria against which antibiosis was tested (Fig. 7).

The same 11 actinobacterial isolates, which had inhibited the growth of foreign mesophilic bacteria, also inhibited at least one or more non-actinobacterial TMA isolate(s) (Fig. 7). *Microbacterium* TW_SC_2 could inhibit the most number of TMA bacteria (nine) outside Actinomycetota. In contrast, *Arthrobacter* TRD_SC_6 could inhibit only one TMA bacterium outside Actinomycetota. From the reverse perspective, every non-actinobacterial TMA isolate was inhibited by at least three TMA actinobacteria. *Aeromonas* TS_SC_11 was the most vulnerable TMA bacteria outside Actinomycetota as its growth was inhibited by 11 TMA actinobacteria. In contrast, *Ancylobacter* TW_SC_1, *Flavobacterium* TS_SC_2, *Pseudomonas* TS_SC_12 and *Pseudomonas* TS_SC_13 were least prone to antibiosis as each of them was susceptible to only three actinobacterial isolates.

Out of the 15 TMA species belonging to Actinomycetota, eight could inhibit the growth of fellow actinobacterial isolates (Fig. 7). Overall, *Microbacterium* TRD_SC_10 and *Pseudarthrobacter* TRD_SC_9 inhibited the most number of actinobacteria (six each). In contrast, *Arthrobacter* TRD_SC_6, and *Microbacterium* TW_SC_2, inhibited only one TMA actinobacteria each. From the opposite point of view, 11 TMA actinobacteria were prone to inhibition by isolates belonging to the same phylum (Fig. 7). *Arthrobacter* TRD_SC_8 (inhibited

by six TMA actinobacteria) was the most vulnerable TMA isolate belonging to Actinomycetota. In contrast, *Microbacterium* TW_SC_3, *Pseudarthrobacter* TRD_SC_9, *Paenarthrobacter* TRD_SC_7 and *Microbacterium* TRD_SC_10, were not prone to inhibition by any of the actinobacterial isolates.

In the context of antibiosis it was further noteworthy that none of the non-actinobacterial species isolated from the TMA could inhibit the growth of any other TMA isolate, whatever may be its phylum affiliation (Fig. 7).

Key attributes of the whole genomes sequenced for selected TMA isolates

Complete whole genome sequence was determined for selected isolates from across the three environments explored within the Tso Moriri lake-desert ecosystem (Table 1). While one genome was sequenced from each of the 15 genera across which the 27 species-level isolates were classified, it was also ensured that at least one strain was analyzed from each cluster that had formed on the basis of growth or population-level survival at different incubation temperatures (Fig. 6a).

De novo hybrid assembly of the short and long DNA sequence reads generated using two different technologies yielded complete or near-complete genome sequences for all the TMA isolated analyzed (Tables 1 and S37). For 10 out of the 15 TMA isolates selected, their complete genomes were encompassed in single circular chromosomes: *Arthrobacter* TRD_SC_6, *Cryobacterium* TS_SC_7, *Flavobacterium* TS_SC_5, *Microbacterium* TW_SC_2, *Mycetocola* TRD_SC_2, *Paenarthrobacter* TRD_SC_7, *Pseudarthrobacter* TRD_SC_9, *Pseudomonas* TS_SC_3, *Sanguibacter* TS_SC_8 and *Trichococcus* TS_SC_9. For two TMA isolates their complete genomes were incorporated in single circular chromosomes plus multiple circular plasmids: *Acinetobacter* TW_SC_4 had two such plasmids of 18.1 kb and 81.9 kb length, while *Psychrobacter* TS_SC_6 had three of them, 6.4 kb, 7.1 kb and 23.1 kb in length. For *Aeromonas* TS_SC_11, *Ancylobacter* TW_SC_1 and *Streptomyces* TRD_SC_5, their near-complete genomes encompassed one or two uncircularized chromosomes plus one or two circular plasmids varying between 43.2 kb and 89 kb in length.

Gene contents of TMA isolates concerned with adaptation to temperature extremes

Inspection of the eggNOG-annotated protein-coding gene sequence (CDS) catalogs of the 15 TMA isolates (Tables S38-S52) revealed diverse genes concerned with low and high temperature adaptations (Figs. 8 and 9a; Table S53). Besides a number of cold-adaptation-related genes concerned with cold-shock response and RNA remodeling, membrane fluidity regulation, and

genome maintenance at low temperatures, several such genes were also detected which conferred tandem adaptation to low as well as high temperatures: these encoded chaperones and other protein quality control components, elicited DNA and oxidative stress responses, coded for global transcriptional regulators, or governed biosynthesis and transport of compatible solutes and osmoprotectants.

Streptomyces TRD_SC_5 had the highest number of cold-adaptation-related genes [33], whereas *Acinetobacter* TW_SC_4 and *Psychrobacter* TS_SC_6 had the lowest [15]. So far as the genes involved in dual adaptation to low as well as high temperatures were concerned, *Streptomyces* TRD_SC_5 [93] and *Psychrobacter* TS_SC_6 [37] had the highest and lowest numbers of them, respectively.

The species isolated from weathered rock dust contained slightly higher diversities of genes [17-33 in number] for cold adaptation (Fig. 9b), compared with the isolates from lake-water [15-25 genes] and lake-sediment [15-25 genes]. Specifically, the *desKR* (KEGG orthology numbers: K07778 and K07693) two-component regulatory system, which controls membrane fluidity amid decreasing temperature (via modulation of fatty acid desaturase gene expression), was possessed mostly by rock-dust isolates (Table S53).

The species isolated from weathered rock dust also possessed relatively higher diversity of genes [44-93 in number] for dual adaptation to low and high temperatures, compared with the lake-water and lake-sediment isolates which possessed 44-58 and 37-59 such genes respectively (Fig. 9c). Specifically, the *treYZ* genes (K06044 and K01236) synthesizing the heat or cold, desiccation, and oxidative stress protectant trehalose; the *opuA*, *opuBD* and *opuC* genes (K05847, K05846 and K05845) governing the uptake of compatible solutes from the environment; and the *ectABC* genes (K06718, K00836 and K06720) synthesizing the protective compatible solute ectoine were possessed almost exclusively by the rock-dust isolates (Table S53).

Genes encoding carbohydrate-active enzymes (CAZymes)

When the CDS catalogs of the selected TMA isolates (Tables S38-S52) were searched against the dbCAN3 and CAZy databases, a wide array of carbohydrate-active enzymes concerned with polysaccharide binding, modification, and degradation were revealed (Table S54). Amid a heterogeneous and overlapping distribution of genes across species isolated from the three TMA habitats, most number of putative CAZymes [293] was encoded by the genome of *Streptomyces* TRD_SC_5, whereas the least number of them [81] was encoded by *Psychrobacter* TS_SC_6. Overall, the detected CAZymes belonged to six broad functional categories - glycoside hydrolase (GH), glycosyl transferase (GT), carbohydrate esterase, polysaccharide lyase, enzymes with

auxiliary activities, and carbohydrate-binding module (Fig. 10a). Of the different classes, again, GH and GT accounted for the most number of genes in all the genomes analyzed (collectively, 67-86% of all CAZyme genes possessed by the different strains were GHs and GTs). That said, most of the TMA isolates that were rich in GHs were relatively poorer in GT diversity, and vice versa. Only *Streptomyces* TRD_SC_5 had equal number of GH and GT genes, while *Microbacterium* TW_SC_2, *Arthrobacter* TRD_SC_6 and *Mycetocola* TRD_SC_2 also had comparable numbers of GH and GT genes. Overall, no clear environment- or habitat-specific trend was apparent when the species-wise distribution of CAZyme genes was considered in the context of the isolation source of the species (Fig. 10b).

Genes encoding antibiotics and other secondary metabolites

Overall, five classes of antibiotics [(i) penicillins and cephalosporins, (ii) prodigiosins, (iii) staurosporines, (iv) tetracyclines and (v) vancomycins; Table S55], and nine classes of secondary metabolites [(i) NI-siderophores, i.e. siderophores independent of non-ribosomal peptide synthase (NRPS), (ii) NAPAAs, i.e. non-alpha poly-amino acids, (iii) Class-II lanthipeptides, (iv) Class-III lanthipeptides, (v) NRPs, or non-ribosomal peptides, (vi) NRP-metallophores, (vii) terpenes, (vii) Type-I polyketides, and (ix) Type-III polyketides, all of which can potentially act as antimicrobial agents (Table S56)] were putatively synthesized by the 15 TMA isolates for which whole genome sequences were analyzed (Table 2).

Every actinobacterium that was capable of inhibiting the growth of one or more target organism(s), and for which the complete whole genome sequence was analyzed, apparently possessed the ability to synthesize one or more classes of known antibiotic(s) and/or secondary metabolite(s). Among all the 15 isolates for which genomes were analyzed, highest diversity of antibiotics and secondarily metabolites was putatively synthesized by the actinobacterium *Streptomyces* TRD_SC_5 (this organism possessed key genes for the synthesis of Class-II and Class-III lanthipeptides, non-ribosomal peptides, siderophores independent of non-ribosomal peptide synthase, staurosporines, terpenes, Type-I polyketides and vancomycins). *Cryobacterium* TS_SC_7 (prodigiosins, NAPAAs, terpenes, and Type-III polyketides), *Paenarthrobacter* TRD_SC_7 (NAPAAs, NI-siderophores, NRPs, and penicillins and cephalosporins), and *Pseudarthrobacter* TRD_SC_9 (NAPAAs, NI-siderophores, staurosporines, and Type-III polyketides) possessed key genes for the synthesis of the next highest diversities of antibiotics and secondarily metabolites. Incidentally, these four actinobacteria had inhibited the growth of 14, 9, 15 and 20 out of the total 33 allochthonous and autochthonous microorganisms against which antibiosis was tested (Fig. 7). *Microbacterium* TW_SC_2 did not have genes

required for the synthesis of any known antibiotic or secondary metabolite other than Type-III polyketides, but it had inhibited the growth of 14 target organisms (Fig. 7), presumably by hitherto unknown antimicrobial agents. On the flip side of the above data, no known antibiotic or secondarily metabolite was apparently synthesized by *Acinetobacter* sp. TW_SC_4, *Pseudomonas* sp. TS_SC_3 and *Psychrobacter* sp. TS_SC_6, which also had shown no antibiosis against any of the 33 targets tested. *Aeromonas* TS_SC_11, *Ancylobacter* TW_SC_1, *Flavobacterium* TS_SC_5, and *Trichococcus* TS_SC_9 too had not inhibited any target organism; corroboratively, they did not also synthesize any known antibiotic (the four species, however, putatively synthesizied a few classes of secondary metabolites; Table 2).

Genes conferring potential resistance against antibiotics

Of the 15 isolates for which genomes were analyzed, only five were found to posssess genes central to resistance against carbapenems, cephalosporins, diaminopyrimidines, elfamycins, fluoroquinolones, penicillins and other beta-lactams, phenicols, rifamycins, teicoplanins, and/or vancomycins (Tables 2 and S57). The remaining 10 genomes were found to encompass no such gene which is central to resistance against any known antibiotic. While potential resistance against rifamycins was accounted for by the highest number of genomes (three), putative resistance against highest number of antibiotic groups was possessed by *Aeromonas* TS_SC_11. This isolate, however, was inhibited by several actinobacterial isolates, apparently by antimicrobials other than penicillins or other beta-lactams, carbapenems, cephalosporins and elfamycins, against which TS_SC_11 possessed putative resistance according to the genomic data (Fig. 7; Table 2).

DISCUSSION

Habitat as the key driver of adaptation to extremes of temperature

All the genera under which the TMA isolates were classified, excepting *Ancylobacter* and *Paenarthrobacter*, encompassed multiple members retrieved previously from other natural or artificial cold/frigid environments (Table S58; also see Supplementary References). Remarkably, each of them also encompassed at least one member retrieved previously from a mesic/hot habitat (Table S59; also see Supplementary References). Consistent with these facts, cell populations of different TMA isolates belonging to the same genus were found to exhibit differential growth/survival at a given incubation temperature (Fig. 6a).

Native environments of the TMA isolates, rather than their phylogenetic background, seemed to exert the most crucial influence on adaptation to extremes of temperature. For all the genera isolated in this study, except *Paenarthrobacter*, member strains from other parts of the world, especially mesic/hot environments, are known to grow at temperatures higher than the maxima recorded for the TMA counterparts (Fig. S5; Table S60; also see Supplementary References). As for *Paenarthrobacter*, it was intriguing as to why the growth temperature maxima of its strains reported earlier from warmer habitats, and that of the current isolate from cold/frigid environment, converged at 37°C. It was, however, understandable that the growth temperature minimum of *Paenarthrobacter* (Fig. S5; Table S60) was pegged thus far at 4°C (42, 43) because no member of this genus had been isolated from any cold habitat before this study. With regard to variable cold adaptation in closely-related bacteria, it was further noteworthy that none of the genera isolated from Tso Moriri area, except *Cryobacterium*, *Pseudomonas*, *Psychrobacter* and *Sanguibacter* (44-47), encompassed any such strain from any other part of the world which possessed growth temperature minimum lower than its TMA counterpart (Fig. S5; Table S60).

Certain common phenotypes seemed to unify majority of strains isolated from a given TMA environment (Fig. 6b).

(1) All the bacteria isolated from the weathered rock dust of the lake-adjoining hill, with the exception of only *Arthrobacter* TRD_SC_4 and TRD_SC_6, grew or survived at the population-level through the entire temperature range tested (i.e. -10°C to 42°C).

(2) The bacteria from Tso Moriri's water also accomplished population-level growth or survival through the entire range of incubation temperatures tested.

(3) Most strains isolated from Tso Moriri's sediment had population-level growth/survival across narrower ranges of incubation temperature, compared to the isolates from rock-dust and lake-water.

Concurrent with the above phenotypic trends, cumulative diversity of genes concerned with all forms of extreme temperature adaptation was relatively higher in the rock-dust and lake-water isolates, compared to those from the lake-sediment (Fig. 9a; Table S53). Individually also, the diversity of genes concerned with adaptation to low (Fig. 9b; Table S53), and low as well as high (Fig. 9c; Table S53), temperatures were relatively higher in the rock-dust and lake-water isolates, compared to those from the lake-sediment.

Tso Moriri's surficial water freezes in the winter and thaws in the summer. Likewise, the rocky slopes of the adjoining hills get covered by snow in the winter and the same melts through the summer; furthermore, the rocks are exposed to extreme heating and cooling on a diurnal basis. Thus, wider temperature windows for population-level growth/survival, and enrichment of

corresponding genetic resources, in bacteria from these two environments could be reflective of a positive linkage between adaptation to the extremes of temperature and the variability of the thermal condition prevailing in the habitat. By the flip side of the same reasoning, it was also quite natural for the bacteria from Tso Moriri's subsurface to have narrower temperature windows (and genes for all forms of extreme temperature adaptation) for population-level growth/survival, compared to their surficial neighbors.

In the context of environment as a key driver of low temperature adaptation, it was further noteworthy that for *Acinetobacter*, *Aeromonas*, *Microbacterium*, *Paernarthrobcter*, *Pseudarthrobacter* and *Trichococcus*, strains known to grow at genus-specific minimum temperatures before this study (Fig. S5; Table S60) were all isolated from mesic or hot environments (42, 48-52), even though other strains of all these genera except *Paenarthrobacter* had been isolated from natural and/or artificial cold/frigid environments (Table S58). On the flip side, strains of *Aeromonas* and *Mycetocola* that were known to grow at genus-specific temperature maxima before this study (Fig. S5; Table S60) were all isolated from natural or artificial cold/frigid environments (53, 54), even though other strains of these genera had been isolated from mesic or hot environments (Table S59). These habitat-phenotype mismatches could be the upshots of drastic microbial transportation across physicochemically distinct ecosystems, alongside the existence of some hitherto unappreciated metabolic convergence between high and low temperature adaptations. Such a counterintuitive idea was reinforced by the facts that out of the 20 cryo-adapted (-10°C-growing) bacteria isolated from the TMA, 16 and 10 could grow at 28°C and 37°C respectively (Fig. 6a). Furthermore, after 1 day at 42°C, only eight TMA isolates had >0.1% CFU left in the culture (Figs. 4f and 4i), and among these, six could also grow at -10°C (Fig. 2b).

Autochthonous populations of heat-susceptible psychrophiles as biogeothermometers of *in situ* warming

TMA isolates, irrespective of their phylogenetic affinities, exhibited different levels of thermal susceptibility. For instance, almost all cells of *Cryobacterium* TS_SC_7 lost their divisibility, as well as metabolic activity, after a four-day exposure to 28°C (Figs. 4b and 4g), so their retrieval from the lake's sediment could be indicative of the fact that the temperature of this under-water substratum either does not reach 28°C, or even if it does so, it does not remain at that level for several days. On the flip side, elimination of such bacteria from environments where they had been prevalent previously would indicate protracted *in situ* warming up to and above 28°C. Population dynamics of TS_SC_7-like bacteria can, therefore, be construed and contrived as

spatiotemporal biogeothermometers of cold/frigid environments that are indisposed to prolonged physical monitoring.

Almost all cells of *Flavobacterium* TS_SC_5 and TS_SC_2 lost their metabolic activity after a full day at 42°C *in vitro* (Figs. 4f and 4i), while their divisibility was already abolished after a single day's exposure to 37°C (Fig. 4c), or even after a two-day exposure to 28°C (Fig. 4a). Likewise, almost all cells of *Arthrobacter* TRD_SC_4 lost their activity after a full day at 42°C (Figs. 4f and 4i), while their divisibility was already abolished after a two-day exposure to 37°C (Figs. 4d and 4h), and only a quarter of the cell population retained its divisibility after four days at 28°C (Figs. 4b and 4g). Thus, a progressive decline in the prevalence of a natural population of *Flavobacterium* species similar to TS_SC_5 and TS_SC_2, over time and/or space, can be correlated with a continuing temporal and/or spatial escalation of temperature to 28°C and above. The same for TRD_SC_4-like populations can, in turn, corroborate ongoing spatiotemporal increases of *in situ* temperature to 37°C and above. In the same vein, population dynamics of bacteria like *Arthrobacter* TRD_SC_6 and *Trichococcus* TS_SC_9, within cold/frigid ecosystems, can be used as real-time bellwethers signaling shifts of *in situ* temperature towards 42°C.

A baseline for *in situ* carbon remineralization under cold/frigid conditions

High levels of organotrophic growth were recorded for all the TMA isolates at 4°C; slow but measurable growth also took place for ~75% of them at -10°C (Figs. 2 and 3). How these *in vitro* metabolic abilities translate into community-level actions *in situ* is central to our knowledge on the baseline of organic matter degradation (carbon remineralization) within the cryosphere. Although biogeochemical data are not yet available for the Tso Morir ecosystem, permeating presence of bacteria similar to the species analyzed genomically was revealed across the three TMA habitats. Small but definite proportions of metagenomic reads obtained from Tso Moriri's water and sediment samples, as well as the sample of weathered rock dust from the lake-side hill, mapped onto each of the 15 whole genomes used as target for sequence alignment. Collectively, the 15 genomes accounted for 0.1%, 0.3% and 0.2% of metagenomic reads from the lake-water, lake-sediment and rock-dust samples respectively (Table S61). These numbers not only illustrated the ubiquity of cryo-adapted and cryo-tolerant copiotrophs similar to the few specimens analyzed here, but also envisaged a biogeochemically effective status for them, across the Tso Moriri ecosystem. Effectiveness of psychrophilic copiotrophs in the biogeochemical cycling (remineralization) of carbon across the Tso Moriri ecosystem was further corroborated by the wide array of carbohydrate-active enzymes detected in the genomes of the current isolates (Fig.

10; Table S54), as well as the assembled metagenomes of the lake-water, lake-sediment, and rock-dust samples (Tables S62).

Thermal susceptibility of autochthonous organotrophs can usher negative feedback control/reversal of warming in cold/frigid ecosystems

Within cold/frigid ecosystems vulnerable to global warming and anthropogenic perturbations (55-57), microbial activity is thought to remain minimal as long as the temperature remains below or around 0°C. However, organic matter degradation, and consequent greenhouse gas emission, starts once *in situ* temperature rises and cryoturbation takes place due to season and/or climate change (58, 59). Increased greenhouse effect brought about by enhanced microbial activities stimulates the biotic processes all the more, and that in turn ushers further thawing via CO_2 and CH_4 emission. In this way, a positive feedback loop of cyclical warming (Fig. 11) is operationalized in the ecosystem (27, 32, 33).

Psychrophilic (4-15°C) growth proficiencies recorded for all the TMA isolates *in vitro*, together with the growth potentials exhibited by most of them at 28°C, indicated that, in nature, microbes-mediated positive feedback cycles can abet environmental warming (via greenhouse gas generation) within the 4°C to 28°C range. On the other hand, above 28°C, gradual cessation of organotrophic growth and activity (Fig. 4) can cut back on the *in situ* production of simple fatty acids and CO_2, which constitute the central substrates of methanogenesis, the terminal process of the carbon cycle (60). Termination of organotrophy, followed by the preemption of methanogenesis, curbs the emission of greenhouse gases, triggers a negative feedback control of warming, and usher over time, a course reversal in the vicious cycle of “warming - microbial growth - and further warming”. Seasonal (winter-mediated) cooling eventually lowers the *in situ* temperature back to the zero and sub-zero degree Celsius levels (Fig. 11).

On the part of a cold/frigid ecosystem, exercise of negative feedback control (termination of autochthonous microbial growth and reduction of metabolic activity; see Fig. 11) towards the restoration of homeostatic balance (reversing the trends of *in situ* warming), is fraught with the danger of indigenous microbes being removed from the habitat, and their ecological niches taken over by more-thermotolerant intruders from discrete geographical territories (Fig. 11). Such incursions can rapidly transform microbiome architectures if not abated at temperatures below the critical level (61) where most cells of most species of the native microflora lose their growth as well as metabolic activity. Potential microbiome transformations can, in the long run, alter ecosystem structures and functions drastically, and in doing so tilt the temperature equilibrium

irreversibly in favour of the positive feedback mechanism (27, 32, 33) which promotes warming (Fig. 11).

Heat-enduring actinobacterial psychrophiles as defenders of cold/frigid microbiomes

In the scenario of an imminent, warming-mediated microbiome alteration, antibiosis potentials of heat-enduring actinobacteria native to the cold/frigid ecosystem (Fig. 7) can deter foreign microbes from colonizing the habitat and apprehending the ecological niches of the indigenous psychrophiles. In the long run, this kind of niche safeguard enhances the chances of population rejuvenation for all autochthonous cold-adapted species upon reversal of thawing (Fig. 11).

Actinomycetota members are known for their extraordinary abilities to produce secondary metabolites including antibiotics, which confer them adaptive fitness against diverse environmental challenges, resulting in the high ecological amplitude of the phylum (62-64). Moreover, they are often abundant in cryospheric microbiomes (65, 66), and are known to protect indigenous microbial communities from external invaders in other critical ecosystems (67). So far as the 15 TMA actinobacteria were concerned, a majority of them were substantially thermotolerant (Figs. 4 and 6a). On top of this, 11 TMA actinobacteria were capable of inhibiting *in vitro* Gram positive and/or Gram negative bacteria from discrete higher-temperature ecosystems at 28°C (Fig. 7), which is lower than the critical high temperature for most of the TMA isolates (Fig. 4). It is, therefore, not unlikely that in the face of plausible microbial incursions from warmer territories, native actinobacterial psychrophiles would thwart foreign occupation and protect indigenous microorganisms from being vanquished from the habitat. Furthermore, in this context it was noteworthy that among the 11 TMA actinobacteria exhibiting antibiosis potentials against foreign bacteria, six had been isolated from the rock-dust sample, while three and two were from the lake's sediment and water respectively (Fig. 7). This showed that microbiome protection by antibiosis-enabled heat-enduring actinobacterial psychrophiles could be widespread across physicochemically distinct cold/frigid environments.

Intricate niche partitioning as central to microbiome functioning within cold/frigid ecosystems

In relation to the broader ecological implications of antibiosis it was noteworthy that a number of TMA actinobacteria eliminated not only foreign microorganisms, but also co-inhabitants of their own environment as well as natives of their adjacent habitats (these included fellow actinobacteria also; see Fig. 7). These findings brought to the fore extensive niche partitioning (68, 69) as a plausible stratagem of microbiome functioning within the cold/frigid ecosystem.

However, neither the phenotypic data, nor the genome-based predictions, available at present in relation to antibiosis (and resistance against the same) could elucidate how ecological niche separation pans out in the micro-environment scale, within the Tso Moriri habitats. In other words, it was not possible from the present data to decipher how niche separation within the TMA habitats effectively precluded direct physical contacts between the actinobacterial antagonists and the species they inhibited *in vitro*. This limitation was attributed to the fact that bulk sampling had already smudged all imprints of niche differentiation, and deciphering of the same would require a new generation of very-finely-resolved spatial study of community ecology.

Genome-based predictions of the TMA isolates' potentials for synthesizing and resisting different antibiotics and secondary metabolites were also not sufficient to elucidate the molecular mechanisms underlying the antibiosis phenotypes recorded *in vitro*. Nevertheless, genomic potentials of the TMA isolates for antibiotic and secondary metabolite synthesis (Table 2) were consistent with their phenotypes recorded in relation to pair-wise antibiosis (Fig. 7). Furthermore, the TMA isolates' antibiotic resistance potentials predicted from genome contents (Table 2) contradicted neither the antibiosis phenotypes recorded *in vitro* nor the genotypes delineated with regard to antibiotics and secondary metabolites synthesis (Table 2). In a nutshell, for every instance where an isolate had inhibited the growth of another TMA species, the antagonist was found to have the genomic potential for synthesizing at least one such class of antibiotic or secondary metabolite against which the inhibited species had no resistance gene.

Using TMA copiotrophs to address the concerns of biodegradation in the cryosphere

Besides global warming, burgeoning human activities have, in recent times, brought about unprecedented perturbations in the delicately balanced cold/frigid ecosystems that are dispersed across the vast high-altitude and high-latitude territories of the world. One of the major factors detrimental to these pristine ecosystems is the accretion of anthropogenic wastes. The pace of microbial growth (19, 26), and thereby degradation of organic matter (26, 70, 71), being slow at temperatures near and below the freezing point of water (also see Figs. 2 and 5), waste-treatment systems (bioreactors) operated in alpine and polar territories require external energy input for optimum-temperature maintenance (72); consequently, these contrivances are neither eco-friendly nor cost effective. Even bioreactors that employ microbes isolated from pristine cold/frigid habitats also sometimes fail to deliver efficient results because psychrophilic microorganisms, owing to their residence in, and adaptation to, organic-carbon-scarce habitats (31, 73), are often oligotrophic in nature (74, 75); accordingly, they are unfit for proliferation in the nutrient-rich environments of bioreactors. Moreover, tens of degree-Celsius thawing above the

freezing point of water runs the risk of making psychrophilic bacterial populations uncompetitive against the thermotolerant, and mostly copiotrophic, microorganisms that find their way into the bioreactors along with the waste materials introduced for degradation (76, 77). In the face of all these challenges, microbes such as the TMA psychrophiles – by virtue of their abilities to (i) grow via catabolism of simple to complex carbon compounds over a wide range of temperature, (ii) grow under low as well as high concentrations of organic matter, and (iii) thwart the proliferation of thermotolerant microbes from warmer habitats – can become ideal constituents of bioreactors designed to perform through zero and sub-zero degree Celsius temperatures.

MATERIALS AND METHODS

Study site

The Himalayas and Trans-Himalayas encompass the largest reservoir of snow and ice on Earth outside the Arctic Circle and Antarctica (78). Within the cold arid vastness of the Himalayan rain shadow, the territory of Ladakh features an extensive high-altitude plateau, where multifaceted microbial life thrives to support homeostatically fragile ecosystems harboring unique multi-stress-adapted plants and animals (28, 79-82). Covering a large swathe of eastern Ladakh (Fig. 1a) sprawls the Changthang desert dotted by several small to large lacustrine bodies among which Tso Moriri is one of the most prominent (Fig. 1b). This gigantic water body (Figs. 1b-c), located at an altitude of 4522 m, is flanked on all sides by barren hills (Figs. 1d-e) that rise either from a distance or very close to the bank of the lake (Fig. 1d). Small patches of lush green meadows, marshes, and wetlands hem only the northern and southwestern shores of Tso Moriri where two big glacial streams pour their water into the lake. Rest of the cold-desert habitat around the lake is characterized by a bleak topography and highly inhospitable physicochemical conditions that are paralleled only by the extreme multi-stressor environments of a few high-altitude areas of the Chilean and Argentinean Andes (83, 84).

Sampling

On 28 October 2021, water (Fig. 1f) and sediment (Fig. 1g) samples were collected from near the western shore of Tso Moriri (at GPS coordinates 32°94′ N and 78°27′ E), together with samples of weathered rock dust from the barren slope of a hill overlooking the western bank of the lake (Fig. 1e). The entire hill slope, rising from ~100 m off the Tso Moriri shore, was devoid of any vegetative cover; visibly, not a single blade of grass grew on it.

In order to arrest the aquatic microbiota, as described previously (85), five different batches of 500 mL water were sampled from five discrete sites located at intervals of 1 m, and within 1 m from the shore of the lake. Each batch of 500 mL water was aspirated from within 1 cm of the lake surface using a sterile syringe (Tarsons Products Limited, India), and passed through an autoclaved, Swinnex holder-mounted (Merck KGaA, Germany), sterile, mixed cellulose ester membrane filter (Merck Life Science Private Limited, India) having a mesh size of 0.22 μm and diameter of 47 mm. Subsequent to filtration, each membrane corresponding to the cell residue of 500 mL lake-water was dislodged from the Swinnex holder, folded using autoclaved forceps, and inserted into a 7.5 mL autoclaved cryovial that contained 5 mL of 15% (v/v) glycerol supplemented with 0.9% (w/v) NaCl (86).

From the same five locations where Tso Moriri's water was sampled, sediments were collected in approximately equal quantities, and pooled inside a single 250 mL polypropylene bottle. Inside the polypropylene bottle the sediment fractions were mixed thoroughly to give rise to a bulk sample which was used for all downstream investigations. At each sampling point, soft deposit was scraped carefully from the sediment-water interface using a flat and wide sterile spatula without disturbing layers deeper than 1 cm from the sediment-surface.

Dry and loose, weathered rock dust samples (fine talus and scree particles) were collected in approximately equal quantities from five distinct points situated within one meter from each other, on the lake-facing slope of the aforesaid hill. At each sampling site, fine powdery materials were scraped cautiously from the surface without disturbing layers deeper than the top 1 cm. The five sample fractions were pooled inside a 250 mL polypropylene bottle, and mixed thoroughly with a sterile spatula to yield a bulk sample that was used for all subsequent investigations.

After the insertion of a cell-precipitated membrane, or sediment / rock-dust sample, each cryovial or polypropylene bottle was capped tightly, sealed with parafilm (Tarsons Products Limited, India), and put inside a polyethylene bag, which eventually was packed in a heat-insulated ice box and shipped by air to the laboratory. All samples were investigated immediately upon their arrival at the laboratory.

In order to extract metagenomic DNA from Tso Moriri's water and sediment, and also from the rock-dust of the lake-side mountain, sampling was carried out as described above. Only for the water sample a few minor adjustments were made. Total 5 L of the lake-water was passed through five separate (pre-autoclaved) 0.22 μm filters (1 L per filter), which in turn were inserted into five different sterilized cryovials, each containing 5 mL of sterile 50 mM Tris:EDTA (pH 7.8).

Enrichment and isolation of cryo-tolerant / cryo-adapted, psychrophilic copiotrophs

In order to enrich copiotrophic, cryo-tolerant / cryo-adapted, psychrophiles from Tso Moriri's water, each 0.22 µm cellulose acetate filter, which contained microbial cell residue from 500 mL lake-water, was shredded with sterile scissors inside the same vial in which it was inserted on-field. The vial was whirled for 15 minutes; after that the filter-shreds were allowed to settle at the bottom; finally, the supernatant was collected in a fresh sterilized vial without disturbing the debris. This process was repeated for all the five filter-containing cryovials involved in lake-water sampling, and the supernatants recovered from each of them were pooled to get an approximately 22 mL cell-suspension in NaCl-glycerol, which corresponded to 2.5 L of bulked lake-water. This ~22 mL cell-suspension was added to 80 mL LB prepared in such a way that the actual nutrient concentrations were achieved after the mixing. The inoculum-medium mixture was subjected to three consecutive cycles of "7 day freezing at -10°C, followed by 7 day thawing at 4°C", after which pure cultures were isolated at an incubation temperature of 4°C by means of dilution plating, picking of visibly-distinct single colonies, and repeated dilution streaking on Luria agar (LA) plates.

To enrich copiotrophic, cryo-tolerant / cryo-adapted, psychrophiles from the lake-sediment or rock-dust sample, 1 g of the corresponding material was added to 100 mL LB, and the suspension was subjected to three cycles of "7 day freezing at -10°C, followed by 7 day thawing at 4°C". After the third round of thawing, pure culture strains were isolated at 4°C in the same way as described above.

All the new isolates were maintained in LA slants with a standard transfer interval of 15 days. For routine growth in LB, or fortnightly transfer in LA, all isolates were grown at 4°C. The strains were classified, as described previously (87), up to the lowest taxonomic rank that was ascribable based on 16S rRNA gene sequence similarities with validly-published species curated in the List of Prokaryotic names with Standing in Nomenclature (88).

Determining the temperature window for growth

The temperature range over which the new isolates could, or could not, grow was delineated by recording the extent to which CFU density increased, or decreased, in the individual LB cultures of the strains, after aerobic incubation at -10°C, 4°C, 15°C, 28°C, 37°C, and 42°C. For a given experiment, a seed culture of the strain tested was prepared by transferring a loopful of cell mass from a 7 day old LA slant culture to fresh 20 mL LB medium kept in a 50 mL Erlenmeyer flask, which was then incubated aerobically at 15°C until when the culture attained its mid-log stage. From this 20 mL seed culture, 1% inoculum was transferred to fresh 20 mL LB medium to set up

the test culture. Experiments checking aerobic growth at incubation temperatures ranging between 4°C and 42°C were carried out in 50 mL Erlenmeyer flasks, whereas those checking aerobic growth at -10°C were carried out in 50 mL polypropylene tubes.

To record CFU density at any time point, 1 mL of the experimental culture concerned was serially diluted using 0.9% (w/v) NaCl, and plated on LA in triplicates (in case of -10°C incubations, the frozen cultures were first liquefied via thawing at 4°C, and then subjected to dilution plating). Subsequently, the LA plates were incubated at 15°C, and colonies appearing on them were counted after 2-3 days depending on the growth rate of the culture in question. Finally, the CFU density was calculated by first multiplying the colony-counts of the individual dilution-plates by their corresponding dilution factors, and subsequently adding and averaging the values across the dilution grades and replica plates available.

The above experiments were repeated for the comparator organism *Escherichia coli* by recording the increases or decreases in CFU density that the LB cultures of strain K-12 underwent after incubation at -10°C, 4°C, 15°C, 28°C, 37°C, and 42°C. *E. coli* seed cultures were prepared in the same as those prepared for the TMA isolates except for the fact that incubations were carried out at 28°C for 12 h. Experimental cultures too were subjected to the same procedure as above, while CFU densities for K-12 were recorded by incubating the colony-counting LA plates at 28°C for two days.

When the final CFU density of an experimental culture recorded after the stipulated period of incubation was higher than its initial (0 hour) CFU density, the growth rate of the concerned isolate, at the temperature in question, was calculated as the percentage change that was recorded in the CFU density over time (percentage of the initial CFU mL^{-1} culture that increased day^{-1} incubation).

$$\text{Growth rate} = \frac{(\text{Final CFU density} - \text{Initial CFU density}) \times 100}{\text{Initial CFU density}} \times \frac{1}{\text{Total days of incubation}}$$

Determining the temperature window for population-level survival

When the final CFU density of an experimental culture recorded after the stipulated period of incubation was lower than its initial (0 hour) CFU density, the survival frequency of the concerned isolate's cell populations at the temperature in question was delineated in terms of what percentage of cells remained metabolically active in the culture. Proportion of metabolically-active cells in a given culture was determined by testing the cells' ability to imbibe the nonfluorescent and nontoxic molecule called fluorescein diacetate (FDA), and subsequently hydrolyze the same

to the tracer compound fluorescein by means of esterase activity (89). Fluorescein-stained cells, eventually, were detected with the help of flow cytometry, as described previously (90, 91).

The procedure of fluorescence-activated cell sorting (FACS) is described below in a nutshell. Cell-pellet was harvested via cold (4°C) centrifugation for 20 minutes at 6000 *g*, and then resuspended in 2 mL of a 0.9% NaCl solution. From a 0.5% (w/v) FDA (Sigma, USA) solution in dimethyl sulfoxide, 4 µl was added to the cell suspension and incubated at 37°C for 15 minutes. The cells were then washed and resuspended again in 500 µl of 0.9% NaCl. Ultimately, with the help of a BD FACSVerse flow cytometer (Becton, Dickinson and Company, USA), 10000 cells were analyzed randomly for their ability to fluoresce through 475-495 nm excitation and 520-530 nm emission. The BD FACSuite software package (Becton, Dickinson and Company) was used to present the data in the form of a dot plot depicting the level of fluorescence recorded for each cell as a function of its photodiode-array-detected ability to forward scatter light having a wave length of 488 nm. Positions of the experiment-specific quadrant gates separating the metabolically-active cells from their inactive counterparts were determined by analyzing an unstained version of the sample.

Testing chemoorganoheterotrophic growth on complex carbon compounds

The TMA isolates were tested for 4°C and -10°C aerobic growth on various simple to complex organic compounds as sole sources of energy, electron, and carbon. For this purpose, each strain was cultured aerobically on modified basal and mineral salts (MS) solution (92) supplemented with any one of the following organic compounds (HiMedia Laboratories, India) at one particular instance (L^{-1} double distilled Milli-Q water): acetate (10 mM), agar (2 g), benzoate (5 mM), cellulose (5 g), chitin (10 g), n-hexadecane (0.5 mL), pectin (10 g), water-soluble starch (4g) and xylan (10 g).

For each experiment, a seed culture of the test strain was prepared by as described above. From the 20 mL seed culture, cells were harvested, then washed twice with 0.9% NaCl, and eventually resuspended in 1 mL MS solution. This cell suspension in MS was added to the test medium (MS solution supplemented with any one of the 10 organic compounds mentioned above) in such a way that the specified concentration of the medium was reached only after the addition of the inoculum (final volume of the test culture was 20 mL). Experiments checking growth at 4°C were carried out in 50 mL Erlenmeyer flasks, whereas those checking growth at -10°C were carried out in 50 mL polypropylene tubes. CFU density of a culture at a given time point of incubation was determined as described for the LB-dependent growth experiments. Furthermore, each of the 27 TMA isolates was tested for its ability to grow in MS solution devoid

of any organic carbon. These experiments were carried out in the same way as described above for testing growth in MS supplemented with a single organic compound,

Testing antibiosis potential

Every TMA isolate was tested by agar overlay assay (93) for its antibiosis potentials against higher-temperature-adapted, mesophilic, Gram negative and Gram positive bacteria that had been isolated previously from warmer habitats within the Western-Himalayan and Trans-Himalayan territories. The Gram negative targets included the well-known model microorganism *Escherichia coli* K-12 (Gammaproteobacteria), plus the temperate soil isolate *Advenella kashmirensis* WT001 that belonged to Betaproteobacteria (94, 95), and the Puga Valley hydrothermal vent isolate *Paracoccus* sp. SMMA_5 that belonged to Alphaproteobacteria (86, 91). The Gram positive targets included the Chumathang hydrothermal vent isolates *Bacillus subtilis* SC_1, *Bacillus licheniformis* PAMA2_SD1, and *Lysinibacillus fusiformis* LAPE1_SD1, all of which belonged to the phylum Bacillota (Dutta et al. unpublished). Each TMA isolate was also tested for its antibiosis capabilities against other isolates obtained from the TMA.

The potential antagonists under assessment (these were taken in batches of four isolates at a time) were first grown in LB, at 15°C for 48 h, to generate their seed cultures. 10 µL inocula from the individual seed cultures were spotted on LA plates at minimum mutual distances of 3 cm, following which the plates were incubated at 15°C for 48 h. After fully grown colonies had appeared for all the potential antagonists investigated, 100 µL of a mid-log-phase culture of the target organism against which antibiosis was to be tested, was mixed with 900 µL molten agar (0.4% w/v) having 37°C temperature, and poured uniformly on the LA plates that were already dotted by incumbent colonies of the potential antagonists. Seed culture of the incoming bacterium (target of potential antibiosis) was grown at 28°C or 15°C, according as the organism was a mesophile from a foreign habitat or an isolate from the TMA. Eventually, these test plates were incubated for 48 h (again, at 28°C or 15°C, according as the incoming bacterium was a mesophile from a foreign habitat or a TMA isolate) and checked for the development of lawns of growth, or clear zones of inhibition, for the incoming organism, around the pre-established colonies of the incumbent bacteria (potential antagonists).

Whole genome extraction, sequencing, and annotation

Whole genomic DNA was extracted from the LB-grown stationary phase culture of a given TMA isolate using HiPurA Bacterial Genomic DNA Purification Kit (Himedia, India), and sequenced using a Novaseq 6000 (Illumina Inc., USA) as well as a MinION (Oxford Nanopore Technologies,

UK) platform. All the read datasets obtained in this way were submitted for public accession to the Sequence Read Archive of National Center for Biotechnology Information (NCBI), USA, under the BioProject PRJNA1335599 (BioSample accession numbers of all the depositions are given in Table S37). For every genome, 2×150 bp paired-end Illumina reads having Phred score above 20 were assembled alongside MinION reads having quality values >10, with the help of the software Unicycler v0.5.0 run in hybrid assembly mode (96). Prodigal v2.6.3 (97) was used to predict open reading frames (ORFs), or putative genes, within the assembled genome. Subsequenly, a catalog of protein-coding gene sequences (CDSs) was delineated by searching the repertoire of ORFs available, against the eggNOG database v5.0 (98), with the aid of eggNOG-mapper v2.1.9 (99), which in turn used the algorithm HMMER.

Identification of genes concerned with the key phenotypes of the TMA isolates

To identify genes associated with low temperature adaptation, and low as well as high temperature adaptation, the eggNOG-derived CDS catalogs of the TMA isolates were searched on the basis of the information available in the literature for extreme temperature adaptation, alongside the gene orthology information curated in the Kyoto Encyclopedia of Genes and Genomes (KEGG; https://www.genome.jp/kegg/).

To identify genes encoding carbohydrate-active enzymes, the Prodigal-derived ORF catalogs of the isolates were annotated directly by searching against the CAZy and dbCAN3 databases using Diamond (100) and HMMER (101) algorithms (with default parameters for both) respectively. Subsequently, the collective findings of the two search exercises were reported as the catalogs of genes encoding carbohydrate-active enzymes.

To identify genes that are known to be central to the biosynthesis of different classes of antibiotics, each eggNOG-derived CDS catalog was searched based on the information available in the literature for antibiotic biosynthesis, plus the gene orthology information curated in the KEGG database. Furhtermore, to detect genes or gene clusters concerned with the biosynthesis of secondary metabolites, each Prodigal-derived ORF catalog was annotated using the bacterial version (v7.0) of the antibiotics and secondary metabolite analysis shell (antiSMASH) pipeline in strict detection mode (102, 103).

Antibiotic resistance genes were identified by annotating the assembled whole genome sequences of the individual TMA isolates against the Comprehensive Antibiotic Resistance Database (CARD, version 3.2.8) using the Resistance Gene Identifier (RGI, version 6.0.3) tool with its default analysis parameters (104).

Metagenomics

From the lake-water, lake-sediment, and rock-dust samples, metagenomic DNA was extracted, and sequenced on a Novaseq 6000 using 2 × 250 bp paired-end read chemistry, as described previously (85, 105). After clipping the adapters and quality-filtering for an average Phred score ≥20, 25,000,000 read-pairs were extracted randomly from each metagenomic sequence dataset and assembled *de novo* using Megahit v1.2.9 with default parameters (106).

Within the >1000 bp contigs assembled from a given metagenome, ORFs or putative genes were annotated using Prodigal v2.6.3 in default mode (107). CAZyme-encoding genes were identified within the gene catalog obtained by searching against the CAZy and dbCAN3 databases using Diamond (100) and HMMER (101) with default parameters respectively. The collective findings of the two searches were eventually reported as the catalog of genes encoding CAZymes within the metagenome in question.

To get an idea about the habitat-wise prevalence (relative abundance) of the different TMA species for which whole genomes were sequenced, the proportion of sequence correspondence that existed between a given genome and the metagenome of the habitat under consideration was determined as follows. First, a subject (target) database was created by curating all the 15 whole genome sequences in hand; subsequently, all Q20 metagenomic reads available for a given habitat were mapped onto the subject database using Bowtie2 v2.4.5 in default mode (108). The alignment output file obtained was processed with SAMtools v 1.13 (109) to report the number of metagenomic reads that matched each genome of the target database individually.

ACKNOWLEDGEMENTS

Extensive on-field assistance provided by Sri Asgar Ali of Choglamsar, Ladakh, India is gratefully acknowledged. We thank Dr. Soumya Chatterjee, Biodegradation Technology Division, Defence Research Laboratory, India, for valuable discussions on cold-customized bioreactors.

FUNDING

The study was financed by Bose Institute through Intramural Research Grants. S.C. and M.M. received fellowships from Department of Biotechnology (DBT), Government of India (GoI). S.D. and J.S. obtained their fellowships from Council of Scientific and Industrial Research, GoI. J. G. and S. S. got fellowships from University Grants Commission, GoI. NM received fellowship from Bose Institute. Bioinformatic analyses were carried out using computational resources available under an EMR project funded by DBT, GoI (BT/PR40174/BTIS/137/45/2022).

AUTHOR CONTRIBUTIONS

W.G. conceived the study, designed the experiments, interpreted the results, and wrote the paper. S.C. anchored the program, planned and performed the experiments, analyzed and curated the data, and also composed the paper. S.D. analyzed the data, while S.D., J.G., S.S., M.M., J.S., and N.M. performed the experiments. All authors read and approved the manuscript.

COMPETING INTEREST

The authors declare no competing interest.

SUPPLEMENTARY DATA

Supplementary information and data are available online in the form of a Word file named Supplimentary_Information.docx, and an Excel file named Supplimentary_Dataset.xlsx.

DATA AVAILABILITY

GenBank accession numbers for the 16S rRNA genes of the new isolates are as follows:

PV789631 (*Arthrobacter* sp. TRD_SC_1), PV789699 (*Arthrobacter* sp. TRD_SC_3), PV789726 (*Arthrobacter* sp. TRD_SC_4); PV789747 (*Arthrobacter* sp. TRD_SC_6); PV789751 (*Arthrobacter* sp. TRD_SC_8); PV793422 (*Cryobacterium* sp. TS_SC_7); PV790046 (*Microbacterium* sp. TRD_SC_10); PV793448 (*Microbacterium* sp. TW_SC_2); PV793500 (*Microbacterium* sp. TW_SC_3); PV789771 (*Mycetocola* sp. TRD_SC_2); PV682789 (*Paenarthrobacter* sp. TRD_SC_7); PV790021 (*Pseudarthrobacter* sp. TRD_SC_9); PV793432 (*Pseudarthrobacter* sp. TS_SC_4); PV793425 (*Sanguibacter* sp. TS_SC_8); PV789776 (*Streptomyces* sp. TRD_SC_5); PV793427 (*Trichococcus* sp. TS_SC_9); PV793436 (*Flavobacterium* sp. TS_SC_2); PV793440 (*Flavobacterium* sp. TS_SC_5); PV790452 (*Ancylobacter* sp. TW_SC_1); PV793444 (*Acinetobacter* sp. TW_SC_4); PV793419 (*Aeromonas* sp. TS_SC_11); PV793374 (*Pseudomonas* sp. TS_SC_1); PV793375 (*Pseudomonas* sp. TS_SC_3); PV793377 (*Pseudomonas* sp. TS_SC_10); PV793378 (*Pseudomonas* sp. TS_SC_12); PV793393 (*Pseudomonas* sp. TS_SC_13); PV793413 (*Psychrobacter* sp. TS_SC_6).

All genome and metagenome sequence data have been deposited to the NCBI under the BioProject accession number PRJNA1335599.

Sequence read datasets for the genomes have been deposited to the Sequence Read Archive (SRA), while the assembled whole genome sequences have been deposited to the GenBank, under the BioSamples accession numbers SAMN52016225 (*Acinetobacter* sp. TW_SC_4), SAMN52392035 (*Aeromonas* sp. TS_SC_11), SAMN52016223 (*Ancylobacter* sp. TW_SC_1),

SAMN52016228 (*Arthrobacter* sp. TRD_SC_6), SAMN52016222 (*Cryobacterium* sp. TS_SC_7), SAMN52392036 (*Flavobacterium* sp. TS_SC_5), SAMN52016224 (*Microbacterium* sp. TW_SC_2), SAMN52016227 (*Mycetocola* sp. TRD_SC_2), SAMN52392037 (*Paenarthrobacter* sp. TRD_SC_7), SAMN52016226 (*Pseudarthrobacter* sp. TRD_SC_9), SAMN52016221 (*Pseudomonas* sp. TS_SC_3), SAMN52392038 (*Psychrobacter* sp. TS_SC_6), SAMN52016220 (*Sanguibacter* sp. TS_SC_8), SAMN52392039 (*Streptomyces* sp. TRD_SC_5), and SAMN52392040 (*Trichococcus* sp. TS_SC_9).

Sequence read datasets for the metagenomes have been deposited to the SRA under the BioSamples accession numbers SAMN53833703 (weathered rock dust), SAMN53833704 (lake-water), and SAMN53833705 (lake-sediment).

REFERENCES

1. Cavicchioli R, Thomas T, Curmi PMG. 2000. Cold stress response in archaea. Extremophiles 4:321-331. https://doi.org/10.1007/s007920070001
2. Öquist MG, Sparrman T, Klemedtsson L, Drotz SH, Grip H, Schleucher J, Nilsson M. 2009. Water availability controls microbial temperature responses in frozen soil CO_2 production. Glob Chang Biol 15:2715-2722. https://doi.org/10.1111/j.1365-2486.2009.01898.x
3. Cary SC, McDonald IR, Barrett JE, Cowan DA. 2010. On the rocks: the microbiology of Antarctic Dry Valley soils. Nat Rev Microbiol 8:129-138. https://doi.org/10.1038/nrmicro2281
4. Choe YH, Kim M, Lee YK. 2021. Distinct microbial communities in adjacent rock and soil substrates on a high arctic polar desert. Front Microbiol 11:607396. https://doi.org/10.3389/fmicb.2020.607396
5. Finlay K, Leavitt PR, Patoine A, Patoine A, Wissel B. 2010. Magnitudes and controls of organic and inorganic carbon flux through a chain of hard-water lakes on the northern Great Plains. Limnol Oceanogr 55:1551-1564. https://doi.org/10.4319/lo.2010.55.4.1551
6. van der Valk AG. 2012. The Biology of Freshwater Wetlands, 2nd ed. Oxford University Press, Oxford, England. https://doi.org/10.1093/acprof:oso/9780199608942.001.0001
7. Clow DW, Stackpoole SM, Verdin KL, Butman DE, Zhu Z, Krabbenhoft DP, Striegl RG. 2015. Organic carbon burial in lakes and reservoirs of the conterminous United States. Environ Sci Technol 49:7614-7622. https://doi.org/10.1021/acs.est.5b00373
8. Archer SD, De los Ríos A, Lee KC, Niederberger TS, Cary SC, Coyne KJ, Douglas S, Lacap-Bugler DC, Pointing SB. 2017. Endolithic microbial diversity in sandstone and granite from the McMurdo Dry Valleys, Antarctica. Polar Biol 40:997-1006. https://doi.org/10.1007/s00300-016-2024-9
9. Samuels T, Bryce C, Landenmark H, Marie-Loudon C, Nicholson N, Stevens AH, Cockell C. 2020. Microbial weathering of minerals and rocks in natural environments. In: Dontsova K, Balogh-Brunstad Z, Le Roux G (eds) Biogeochemical Cycles: Ecological Drivers and

Environmental Impact. John Wiley & Sons, Inc, Hoboken, NJ, USA, pp 59-79. https://doi.org/10.1002/9781119413332.ch3

10. Hodson A, Anesio AM, Tranter M, Fountain A, Osborn M, Priscu J, Laybourn-Parry J, Sattler B. 2008. Glacial ecosystems. Ecol Monogr 78:41-67. https://doi.org/10.1890/07-0187.1

11. Boetius A, Anesio AM, Deming JW, Mikucki JA, Rapp JZ. 2015. Microbial ecology of the cryosphere: sea ice and glacial habitats. Nat Rev Microbiol 13:677-690. https://doi.org/10.1038/nrmicro3522

12. Yarzábal LA, Salazar LM, Batista-García RA. 2021. Climate change, melting cryosphere and frozen pathogens: Should we worry…?. Environ Sustain 4:489-501. https://doi.org/10.1007/s42398-021-00184-8

13. Cook JM, Tedstone AJ, Williamson C, McCutcheon J, Hodson AJ, Dayal A, Skiles M, Hofer S, Bryant R, McAree O, McGonigle A, Ryan J, Anesio AM, Irvine-Fynn TDL, Hubbard A, Hanna E, Flanner M, Mayanna S, Benning LG, van As D, Yallop M, McQuaid JB, Gribbin T, Tranter M. 2020. Glacier algae accelerate melt rates on the south-western Greenland Ice Sheet. Cryosphere 14:309-330. https://doi.org/10.5194/tc-14-309-2020

14. Williamson CJ, Cook J, Tedstone A, Yallop M, McCutcheon J, Poniecka E, Campbell D, Irvine-Fynn T, McQuaid J, Tranter M, Perkins R, Anesio A. 2020. Algal photophysiology drives darkening and melt of the Greenland Ice Sheet. Proc Natl Acad Sci U S A 117:5694-5705. https://doi.org/10.1073/pnas.1918412117

15. Ma H, Yan W, Xiao X, Shi G, Li Y, Sun B, Dou Y, Zhang Y. 2018. Ex situ culturing experiments revealed psychrophilic hydrogentrophic methanogenesis being the potential dominant methane-producing pathway in subglacial sediment in Larsemann Hills, Antarctic. Front Microbiol 9:237. https://doi.org/10.3389/fmicb.2018.00237

16. Lamarche-Gagnon G, Wadham JL, Sherwood Lollar B, Arndt S, Fietzek P, Beaton AD, Tedstone AJ, Telling J, Bagshaw EA, Hawkings JR, Kohler TJ, Zarsky JD, Mowlem MC, Anesio AM, Stibal M. 2019. Greenland melt drives continuous export of methane from the ice-sheet bed. Nature 565:73-77. https://doi.org/10.1038/s41586-018-0800-0

17. Zhang Y, Kang S, Wei D, Luo X, Wang Z, Gao T. 2021. Sink or source? Methane and carbon dioxide emissions from cryoconite holes, subglacial sediments, and proglacial river runoff during intensive glacier melting on the Tibetan Plateau. Fundam Res 1:232-239. https://doi.org/10.1016/j.fmre.2021.04.005

18. Drotz, Stina Harrysson, Tobias Sparrman, Mats B. Nilsson, Jürgen Schleucher, Mats G. Öquist. 2010. Both catabolic and anabolic heterotrophic microbial activity proceed in frozen soils. Proc Natl Acad Sci U S A 107:21046-21051. https://doi.org/10.1073/pnas.1008885107

19. Nikrad MP, Kerkhof LJ, Häggblom MM. 2016. The subzero microbiome: microbial activity in frozen and thawing soils. FEMS Microbiol Ecol 92:fiw081. https://doi.org/10.1093/femsec/fiw081

20. Verpoorter C, Kutser T, Seekell DA, Tranvik LJ. 2014. A global inventory of lakes based on high-resolution satellite imagery. Geophys Res Lett 41:6396-6402. https://doi.org/10.1002/2014GL060641

21. Kessler MA, Plug LJ, Walter Anthony KM. 2012. Simulating the decadal to millennial scale dynamics of morphology and sequestered carbon mobilization of two thermokarst lakes in N.W. Alaska. J Geophys Res 117:G00M06. https://doi.org/10.1029/2011JG001796

22. MacIntyre S, Cortés A, Sadro S. 2018. Sediment respiration drives circulation and production of CO2 in ice-covered Alaskan arctic lakes. Limnol Oceanogr Lett 3:302-310. https://doi.org/10.1002/lol2.10083

23. Serikova S, Pokrovsky OS, Laudon H, Krickov IV, Lim AG, Manasypov RM, Karlsson J. 2019. High carbon emissions from thermokarst lakes of Western Siberia. Nat Commun 10:1552. https://doi.org/10.1038/s41467-019-09592-1

24. Guo M, Zhuang Q, Tan Z, Shurpali N, Juutinen S, Kortelainen P, Martikainen PJ. 2020. Rising methane emissions from boreal lakes due to increasing ice-free days. Environ Res Lett 15:064008. https://doi.org/10.1088/1748-9326/ab8254

25. Johnston SE, Striegl RG, Bogard MJ, Dornblaser MM, Butman DE, Kellerman AM, Wickland KP, Podgorski DC, Spencer RGM. 2020. Hydrologic connectivity determines dissolved organic matter biogeochemistry in northern high-latitude lakes. Limnol Oceanogr 65:1764-1780. https://doi.org/10.1002/lno.11417

26. Mohn WW, Stewart GR. 2000. Limiting factors for hydrocarbon biodegradation at low temperature in Arctic soils. Soil Biol Biochem 32:1161-1172. https://doi.org/10.1016/S0038-0717(00)00032-8

27. Graham DE, Wallenstein MD, Vishnivetskaya TA, Waldrop MP, Phelps TJ, Pfiffner SM, Onstott TC, Whyte LG, Rivkina EM, Gilichinsky DA, Elias DA, Mackelprang R, VerBerkmoes NC, Hettich RL, Wagner D, Wullschleger SD, Jansson JK. 2012. Microbes in thawing permafrost: the unknown variable in the climate change equation. ISME J 6:709-712. https://doi.org/10.1038/ismej.2011.163

28. Aschenbach K, Conrad R, Řeháková K, Doležal J, Janatková K, Angel R. 2013. Methanogens at the top of the world: occurrence and potential activity of methanogens in newly deglaciated soils in high-altitude cold deserts in the Western Himalayas. Front Microbiol 4:359. https://doi.org/10.3389/fmicb.2013.00359

29. Ernakovich JG, Wallenstein MD, Calderón FJ. 2015. Chemical indicators of cryoturbation and microbial processing throughout an Alaskan permafrost soil depth profile. Soil Sci Soc Am J 79:783-793. https://doi.org/10.2136/sssaj2014.10.0420

30. Walz J, Knoblauch C, Böhme L, Pfeiffer EM. 2017. Regulation of soil organic matter decomposition in permafrost-affected Siberian tundra soils-Impact of oxygen availability, freezing and thawing, temperature, and labile organic matter. Soil Biol Biochem 110:34-43. https://doi.org/10.1016/j.soilbio.2017.03.001

31. Zimov SA, Schuur EA, Chapin FS III. 2006. Permafrost and the global carbon budget. Science 312:1612-1613. https://doi.org/10.1126/science.1128908

32. Walter KM, Zimov SA, Chanton JP, Verbyla D, Chapin III FS. 2006. Methane bubbling from Siberian thaw lakes as a positive feedback to climate warming. Nature 443:71-75. https://doi.org/10.1038/nature05040

33. Schneider von Deimling T, Meinshausen M, Levermann A, Huber V, Frieler K, Lawrence DM, Brovkin V. 2012. Estimating the near-surface permafrost-carbon feedback on global warming. Biogeosciences 9:649-665. https://doi.org/10.5194/bg-9-649-2012

34. Cavicchioli R. 2006. Cold-adapted archaea. Nat Rev Microbiol 4:331-343. https://doi.org/10.1038/nrmicro1390

35. Cavicchioli R. 2016. On the concept of a psychrophile. ISME J 10:793-795. https://doi.org/10.1038/ismej.2015.160

36. Raymond-Bouchard I, Goordial J, Zolotarov Y, Ronholm J, Stromvik M, Bakermans C, Whyte LG. 2018. Conserved genomic and amino acid traits of cold adaptation in subzero-growing Arctic permafrost bacteria. FEMS Microbiol Ecol 94:fiy023. https://doi.org/10.1093/femsec/fiy023

37. Hubert C, Loy A, Nickel M, Arnosti C, Baranyi C, Brüchert V, Ferdelman T, Finster K, Christensen FM, Rosa de Rezende J, Vandieken V, Jørgensen BB. 2009. A constant flux of diverse thermophilic bacteria into the cold Arctic seabed. Science 325:1541-1544. https://doi.org/10.1126/science.1174012

38. Pearce DA, Bridge PD, Hughes KA, Sattler B, Psenner R, Russell NJ. 2009. Microorganisms in the atmosphere over Antarctica. FEMS Microbiol Ecol 69:143-157. https://doi.org/10.1111/j.1574-6941.2009.00706.x

39. Emara HI. 1998. Total organic carbon content in the waters of the Arabian Gulf. Environ int 24:97-103. https://doi.org/10.1016/S0160-4120(97)00125-6

40. Bhattacharya S, Mapder T, Fernandes S, Roy C, Sarkar J, Rameez MJ, Mandal S, Sar A, Chakraborty AK, Mondal N, Chatterjee S, Dam B, Peketi A, Chakraborty R, Mazumdar A, and Ghosh W. 2021. Sedimentation rate and organic matter dynamics shape microbiomes across a continental margin. Biogeosciences 18:5203–5222. https://doi.org/10.5194/bg-18-5203-2021

41. Elser JJ, Wu C, González AL, Shain DH, Smith HJ, Sommaruga R, Williamson CE, Brahney J, Hotaling S, Vanderwall J, Yu J. 2020. Key rules of life and the fading cryosphere: Impacts in alpine lakes and streams. Glob Chang Biol 26:6644-6656. https://doi.org/10.1111/gcb.15362

42. Kotoučková L, Schumann P, Durnova E, Spröer C, Sedláček I, Neča J, Zdráhal Z, Němec M. 2004. *Arthrobacter nitroguajacolicus* sp. nov., a novel 4-nitroguaiacol-degrading actinobacterium. Int J Syst Evol Microbiol 54:773-777. https://doi.org/10.1099/ijs.0.02923-0

43. Busse HJ. 2016. Review of the taxonomy of the genus *Arthrobacter*, emendation of the genus *Arthrobacter* sensu lato, proposal to reclassify selected species of the genus *Arthrobacter* in the novel genera *Glutamicibacter* gen. nov., *Paeniglutamicibacter* gen. nov., *Pseudoglutamicibacter* gen. nov., *Paenarthrobacter* gen. nov. and *Pseudarthrobacter*

gen. nov., and emended description of *Arthrobacter roseus*. Int J Syst Evol Microbiol 66:9-37. https://doi.org/10.1099/ijsem.0.000702

44. Molin G, Ternström A, Ursing J. 1986. *Pseudomonas lundensis*, a new bacterial species isolated from meat. Int J Syst Evol Microbiol 36:339-342. https://doi.org/10.1099/00207713-36-2-339

45. Bakermans C, Ayala-del-Río HL, Ponder MA, Vishnivetskaya T, Gilichinsky D, Thomashow MF, Tiedje JM. 2006. *Psychrobacter cryohalolentis* sp. nov. and *Psychrobacter arcticus* sp. nov., isolated from Siberian permafrost. Int J Syst Evol Microbiol 56:1285-1291. https://doi.org/10.1099/ijs.0.64043-0

46. Liu W, Zhou X, Jin T, Li Y, Wu B, Yu D, Yu Z, Su B, Chen R, Feng Y, Delgado-Baquerizo M. 2022. Multikingdom interactions govern the microbiome in subterranean cultural heritage sites. Proc Natl Acad Sci U S A 119:e2121141119. https://doi.org/10.1073/pnas.2121141119

47. Pikuta EV, Lyu Z, Williams MD, Patel NB, Liu Y, Hoover RB, Busse HJ, Lawson PA, Whitman WB. 2017. *Sanguibacter gelidistatuariae* sp. nov., a novel psychrotolerant anaerobe from an ice sculpture in Antarctica, and emendation of descriptions of the family Sanguibacteraceae, the genus *Sanguibacter* and species *S. antarcticus*, *S. inulinus*, *S. kedieii*, *S. marinus*, *S. soli* and *S. suarezii*. Int J Syst Evol Microbiol 67:1442-1450. https://doi.org/10.1099/ijsem.0.001838

48. Krovacek K, Faris A, Månsson I. 1991. Growth of and toxin production by *Aeromonas hydrophila* and *Aeromonas sobria* at low temperatures. Int J Food Microbiol 13:165-175. https://doi.org/10.1016/0168-1605(91)90058-w

49. Pikuta EV, Hoover RB, Bej AK, Marsic D, Whitman WB, Krader PE, Tang J. 2006. *Trichococcus patagoniensis* sp. nov., a facultative anaerobe that grows at -5°C, isolated from penguin guano in Chilean Patagonia. Int J Syst Evol Microbiol 56:2055-2062. https://doi.org/10.1099/ijs.0.64225-0

50. Yamahira K, Hirota K, Nakajima K, Morita N, Nodasaka Y, Yumoto I. 2008. *Acinetobacter* sp. strain Ths, a novel psychrotolerant and alkalitolerant bacterium that utilizes hydrocarbon. Extremophiles 12:729-734. https://doi.org/10.1007/s00792-008-0180-8

51. Kallimanis A, Kavakiotis K, Perisynakis A, Sproer C, Pukall R, Drainas C, Koukkou AI. 2009. *Arthrobacter phenanthrenivorans* sp. nov., to accommodate the phenanthrene-degrading bacterium *Arthrobacter* sp. strain Sphe3. Int J Syst Evol Microbiol 59:275-279. https://doi.org/10.1099/ijs.0.000984-0

52. Paściak M, Pawlik KJ, Martynowski D, Łaczmański Ł, Ciekot J, Szponar B, Wójcik-Fatla A, Mackiewicz B, Farian E, Cholewa G, Cholewa A, Dutkiewicz J. 2024. Discovery of a new bacterium, *Microbacterium betulae* sp. nov., in birch wood associated with hypersensitivity pneumonitis in woodworkers. Environ Microbiol Rep 16:e13311. https://doi.org/10.1111/1758-2229.13311

53. Rouf MA, Rigney MM. 1971. Growth temperatures and temperature characteristics of *Aeromonas*. Appl Microbiol 22:503-506. https://doi.org/10.1128/am.22.4.503-506.1971

54. Zhu L, Liu Q, Liu H, Zhou Y, Xin Y, Dong X. 2013. *Mycetocola miduiensis* sp. nov., a psychrotolerant bacterium isolated from Midui glacier. Int J Syst Evol Microbiol 63:2661-2665. https://doi.org/10.1099/ijs.0.047985-0

55. Forbes BC, Ebersole JJ, Strandberg B. 2001. Anthropogenic disturbance and patch dynamics in circumpolar arctic ecosystems. Conserv Biol 15:954-969. https://doi.org/10.1046/j.1523-1739.2001.015004954.x

56. Aronson RB, Thatje S, McClintock JB, Hughes KA. 2011. Anthropogenic impacts on marine ecosystems in Antarctica. Ann N Y Acad Sci 1223:82-107. https://doi.org/10.1111/j.1749-6632.2010.05926.x

57. Geoffroy M, Bouchard C, Flores H, Robert D, Gjøsæter H, Hoover C, Hop H, Hussey NE, Nahrgang J, Steiner N, Bender M, Berge J, Castellani G, Chernova N, Copeman L, David CL, Deary A, Divoky G, Dolgov AV , Duffy-Anderson J, Dupont N, Durant JM, Elliott K, Gauthier S, Goldstein ED, Gradinger R, Hedges K, Herbig J, Laurel B, Loseto L, Maes S, Mark FC, Mosbech A, Pedro S, Pettitt-Wade H, Prokopchuk I, Renaud PE, Schembri S, Vestfals C, Walkusz W. 2023. The circumpolar impacts of climate change and anthropogenic stressors on Arctic cod (*Boreogadus saida*) and its ecosystem. Elementa 11:00097. https://doi.org/10.1525/elementa.2022.00097

58. Knoblauch C, Beer C, Liebner S, Grigoriev MN, Pfeiffer EM. 2018. Methane production as key to the greenhouse gas budget of thawing permafrost. Nat Clim Chang 8:309-312. https://doi.org/10.1038/s41558-018-0095-z

59. Schuur EA, Abbott BW, Commane R, Ernakovich J, Euskirchen E, Hugelius G, Grosse G, Jones M, Koven C, Leshyk V, Lawrence D, Loranty MM, Mauritz M, Olefeldt D, Natali S, Rodenhizer H, Salmon V, Schädel C, Strauss J, Treat C, Turetsky M. 2022. Permafrost and climate change: Carbon cycle feedbacks from the warming Arctic. Annu Rev Environ Resour 47:343-371. https://doi.org/10.1146/annurev-environ-012220-011847

60. Hedderich R, Whitman WB. 2013. Physiology and biochemistry of the methane-producing archaea. In: Rosenberg E, DeLong EF, Lory S, Stackebrandt E, Thompson F (eds) The Prokaryotes. Springer, Berlin, Heidelberg, Germany, pp 635–662. https://doi.org/10.1007/978-3-642-30141-4_81

61. Kosaka T, Nakajima Y, Ishii A, Yamashita M, Yoshida S, Murata M, Kato K, Shiromaru Y, Kato S, Kanasaki Y, Yoshikawa H, Matsutani M, Thanonkeo P, Yamada M. 2019. Capacity for survival in global warming: Adaptation of mesophiles to the temperature upper limit. PLoS One 14:e0215614. https://doi.org/10.1371/journal.pone.0215614

62. Claverías FP, Undabarrena A, González M, Seeger M, Cámara B. 2015. Culturable diversity and antimicrobial activity of actinobacteria from marine sediments in Valparaíso bay, Chile. Front Microbiol 6:737. https://doi.org/10.3389/fmicb.2015.00737

63. Barka EA, Vatsa P, Sanchez L, Gaveau-Vaillant N, Jacquard C, Klenk HP, Clément C, Ouhdouch Y, van Wezel GP. 2016. Taxonomy, physiology, and natural products of Actinobacteria. Microbiol Mol Biol Rev 80:1-43. https://doi.org/10.1128/mmbr.00019-15

64. Lewin GR, Carlos C, Chevrette MG, Horn HA, McDonald BR, Stankey RJ, Fox BG, Currie CR. 2016. Evolution and Ecology of Actinobacteria and Their Bioenergy Applications. Annu Rev Microbiol 70:235-254. https://doi.org/10.1146/annurev-micro-102215-095748

65. Shen L, Liu Y, Allen MA, Xu B, Wang N, Williams TJ, Wang F, Zhou Y, Liu Q, Cavicchioli R. 2021. Linking genomic and physiological characteristics of psychrophilic *Arthrobacter* to metagenomic data to explain global environmental distribution. Microbiome 9:136. https://doi.org/10.1186/s40168-021-01084-z

66. Voytsekhovskaya IV, Axenov-Gribanov DV, Murzina SA, Pekkoeva SN, Protasov ES, Gamaiunov SV, Timofeyev MA. 2018. Estimation of antimicrobial activities and fatty acid composition of actinobacteria isolated from water surface of underground lakes from Badzheyskaya and Okhotnichya caves in Siberia. PeerJ 6:e5832. https://doi.org/10.7717/peerj.5832

67. Salazar-Hamm PS, Homan FE, Good SA, Hathaway JJ, Clements AE, Haugh EG, Caesar LK. 2025. Subterranean marvels: microbial communities in caves and underground mines and their promise for natural product discovery. Nat Prod Rep 42:592-622. https://doi.org/10.1039/d4np00055b

68. Dussud C, Meistertzheim AL, Conan P, Pujo-Pay M, George M, Fabre P, Coudane J, Higgs P, Elineau A, Pedrotti ML, Gorsky G, Ghiglione JF. 2018. Evidence of niche partitioning among bacteria living on plastics, organic particles and surrounding seawaters. Environ Pollut 236:807-816. https://doi.org/10.1016/j.envpol.2017.12.027

69. Shaiber A, Willis AD, Delmont TO, Roux S, Chen LX, Schmid A, Yousef M, Watson AR, Lolans K, Esen ÖC, Lee ST, Downey N, Morrison HG, Dewhirst FE, Mark Welch JL, Eren AM. 2020. Functional and genetic markers of niche partitioning among enigmatic members of the human oral microbiome. Genome Biol 21:1-35. https://doi.org/10.1186/s13059-020-02195-w

70. Gupta SK, Kataki S, Chatterjee S, Prasad RK, Datta S, Vairale MG, Sharma S, Dwivedi SK, Gupta DK. 2020. Cold adaptation in bacteria with special focus on cellulase production and its potential application. J Clean Prod 258:120351. https://doi.org/10.1016/j.jclepro.2020.120351

71. Si-Zhong YA, Hui-Jun JI, Zhi WE, Rui-Xia HE, Yan-Jun JI, Xiu-Mei LI, Shao-Peng YU. 2009. Bioremediation of oil spills in cold environments: a review. Pedosphere 19:371-381. https://doi.org/10.1016/S1002-0160(09)60128-4

72. Dhaked RK, Singh P, Singh L. 2010. Biomethanation under psychrophilic conditions. Waste Manag 30:2490-2496. https://doi.org/10.1016/j.wasman.2010.07.015

73. Schuur EA, McGuire AD, Schädel C, Grosse G, Harden JW, Hayes DJ, Hugelius G, Koven CD, Kuhry P, Lawrence DM, Natali SM, Olefeldt D, Romanovsky VE, Schaefer K, Turetsky MR, Treat CC, Vonk JE. 2015. Climate change and the permafrost carbon feedback. Nature 520:171-179. https://doi.org/10.1038/nature14338

74. Gilichinsky D, Vishnivetskaya T, Petrova M, Spirina E, Mamykin V, Rivkina E. 2008. Bacteria in Permafrost. In: Margesin R, Schinner F, Marx JC, Gerday C (eds)

Psychrophiles: from Biodiversity to Biotechnology. Springer, Berlin, Heidelberg, Germany, pp 83-102. https://doi.org/10.1007/978-3-540-74335-4_6

75. Zhang DC, Brouchkov A, Griva G, Schinner F, Margesin R. 2013. Isolation and characterization of bacteria from ancient siberian permafrost sediment. Biology (Basel) 2:85-106. https://doi.org/10.3390/biology2010085

76. García-Descalzo L, García-López E, Cid C. 2022. Comparative proteomic analysis of psychrophilic vs. mesophilic bacterial species reveals different strategies to achieve temperature adaptation. Front Microbiol 13:841359. https://doi.org/10.3389/fmicb.2022.841359

77. Piercy E, Sun X, Ellis PR, Taylor M, Guo M. 2025. Temporal dynamics of microbial communities in anaerobic digestion: Influence of temperature and feedstock composition on reactor performance and stability. Water Res 284:123974. https://doi.org/10.1016/j.watres.2025.123974

78. Meena V, Kukreja S. 2025. The Third Pole at risk: how climate change is impacting the Himalayas. IORA Ecological Solutions. Accessed 10 July 2025. https://ioraecological.com/the-third-pole-at-risk-how-climate-change-is-impacting-the-himalayas

79. Dvorský M, Doležal J, De Bello F, Klimešová J, Klimeš L. 2011. Vegetation types of East Ladakh: species and growth form composition along main environmental gradients. Appl Veg Sci 14:132-147. https://doi.org/10.1111/j.1654-109X.2010.01103.x

80. Dvorský M, Doležal J, Kopecký M, Chlumska Z, Janatková K, Altman J, de Bello F, Řeháková K. 2013. Testing the stress-gradient hypothesis at the roof of the world: effects of the cushion plant *Thylacospermum caespitosum* on species assemblages. PLoS One 8:e53514. https://doi.org/10.1371/journal.pone.0053514

81. Janatková K, Řeháková K, Doležal J, Šimek M, Chlumská Z, Dvorský M, Kopecký M. 2013. Community structure of soil phototrophs along environmental gradients in arid Himalaya. Environ Microbiol 15:2505-2516. https://doi.org/10.1111/1462-2920.12132

82. Angel R, Conrad R, Dvorsky M, Kopecky M, Kotilínek M, Hiiesalu I, Schweingruber F, Doležal J. 2016. The root-associated microbial community of the world's highest growing vascular plants. Microb Ecol 72:394-406. https://doi.org/10.1007/s00248-016-0779-8

83. Albarracín VH, Gärtner W, Farias ME. 2016. Forged under the Sun: Life and art of extremophiles from Andean lakes. Photochem Photobiol 92:14-28. https://doi.org/10.1111/php.12555

84. Albarracín VH, Kurth D, Ordoñez OF, Belfiore C, Luccini E, Salum GM, Piacentini RD, Farías ME. 2015. High-up: A remote reservoir of microbial extremophiles in Central Andean wetlands. Front Microbiol 6:1404. https://doi.org/10.3389/fmicb.2015.01404

85. Mondal N, Dutta S, Chatterjee S, Sarkar J, Mondal M, Roy C, Chakraborty R, Ghosh W. 2024. *Aquificae* overcomes competition by archaeal thermophiles, and crowding by bacterial mesophiles, to dominate the boiling vent-water of a Trans-Himalayan sulfur-borax spring. PLoS One 19:e0310595. https://doi.org/10.1371/journal.pone.0310595

86. Roy C, Alam M, Mandal S, Haldar PK, Bhattacharya S, Mukherjee T, Roy R, Rameez MJ, Misra AK, Chakraborty R, Nanda AK, Mukhopadhyay SK, Ghosh W. 2016. Global association between thermophilicity and vancomycin susceptibility in bacteria. Front Microbiol 7:412. https://doi.org/10.3389/fmicb.2016.00412

87. Saha T, Ranjan VK, Ganguli S, Thakur S, Chakraborty B, Barman P, Ghosh W, Chakraborty R. 2019. *Pradoshia eiseniae* gen. nov., sp. nov., a spore-forming member of the family Bacillaceae capable of assimilating 3-nitropropionic acid, isolated from the anterior gut of the earthworm *Eisenia fetida*. Int J Syst Evol Microbiol 69:1265-1273. https://doi.org/10.1099/ijsem.0.003304

88. Parte AC, Sardà Carbasse J, Meier-Kolthoff JP, Reimer LC, Göker M. 2020. List of Prokaryotic names with Standing in Nomenclature (LPSN) moves to the DSMZ. Int J Syst Evol Microbiol 70:5607-5612. https://doi.org/10.1099/ijsem.0.004332

89. Battin TJ. 1997. Assessment of fluorescein diacetate hydrolysis as a measure of total esterase activity in natural stream sediment biofilms. Sci Total Environ 198:51-60. https://doi.org/10.1016/S0048-9697(97)05441-7

90. Samaddar S, Grewal RK, Sinha S, Ghosh S, Roy S, Das Gupta SK. 2016. Dynamics of mycobacteriophage-mycobacterial host interaction-evidence for secondary mechanisms for host lethality. Appl Environ Microbiol 82:124-133. https://doi.org/10.1128/AEM.02700-15

91. Mondal N, Roy C, Chatterjee S, Sarkar J, Dutta S, Bhattacharya S, Chakraborty R, Ghosh W. 2022. Thermal endurance by a hot-spring-dwelling phylogenetic relative of the mesophilic *Paracoccus*. Microbiol Spectr 10:e01606-22. https://doi.org/10.1128/spectrum.01606-22

92. Ghosh W, Roy P. 2006. *Mesorhizobium thiogangeticum* sp. nov., a novel sulfur-oxidizing chemolithoautotroph from rhizosphere soil of an Indian tropical leguminous plant. Int J Syst Evol Microbiol 56:91-97. https://doi.org/10.1099/ijs.0.63967-0

93. Berberov K, Atanasova N, Teodosiu-Beleuță G, Boyadzieva I. 2025. Prospecting the biotechnological potential of culturable halophilic bacteria isolated from Provadia salt deposit (Bulgaria) near the oldest salt production and urban complex in Europe. Extremophiles 29:21. https://doi.org/10.1007/s00792-025-01387-1

94. Ghosh W, Alam M, Roy C, Pyne P, George A, Chakraborty R, Majumder S, Agarwal A, Chakraborty S, Majumdar S, Gupta SK. 2013. Genome implosion elicits host-confinement in Alcaligenaceae: evidence from the comparative genomics of *Tetrathiobacter kashmirensis*, a pathogen in the making. PLoS One 8:e64856. https://doi.org/10.1371/journal.pone.0064856

95. Ghosh W, Bagchi A, Mandal S, Dam B, Roy P. 2005. *Tetrathiobacter kashmirensis* gen. nov., sp. nov., a novel mesophilic, neutrophilic, tetrathionate-oxidizing, facultatively chemolithotrophic betaproteobacterium isolated from soil from a temperate orchard in Jammu and Kashmir, India. Int J Syst Evol Microbiol 55:1779-1787. https://doi.org/10.1099/ijs.0.63595-0

96. Wick RR, Judd LM, Gorrie CL, Holt KE. 2017. Unicycler: Resolving bacterial genome assemblies from short and long sequencing reads. PLoS Comput Biol 13:e1005595. https://doi.org/10.1371/journal.pcbi.1005595

97. Hyatt D, Chen GL, Locascio PF, Land ML, Larimer FW, Hauser LJ. 2010. Prodigal: prokaryotic gene recognition and translation initiation site identification. BMC Bioinform 11:119. https://doi.org/10.1186/1471-2105-11-119

98. Huerta-Cepas J, Szklarczyk D, Heller D, Hernández-Plaza A, Forslund SK, Cook H, Mende DR, Letunic I, Rattei T, Jensen LJ, von Mering C, Bork P. 2019. eggNOG 5.0: a hierarchical, functionally and phylogenetically annotated orthology resource based on 5090 organisms and 2502 viruses. Nucleic Acids Res. 47:D309–D314. https://doi.org/10.1093/nar/gky1085

99. Cantalapiedra CP, Hernández-Plaza A, Letunic I, Bork P, Huerta-Cepas J. 2021 eggNOG-mapper v2: functional annotation, orthology assignments, and domain prediction at the metagenomic scale. Mol Biol Evol 38:5825–5829. https://doi.org/10.1093/molbev/msab293

100. Buchfink B, Xie C, Huson DH. 2015. Fast and sensitive protein alignment using DIAMOND. Nat Methods 12:59–60. https://doi.org/10.1038/nmeth.3176

101. Zheng J, Ge Q, Yan Y, Zhang X, Huang L, Yin Y. 2023. dbCAN3: automated carbohydrate-active enzyme and substrate annotation. Nucleic Acids Res 51:W115-21. https://doi.org/10.1093/nar/gkad328

102. Medema MH, Blin K, Cimermancic P, De Jager V, Zakrzewski P, Fischbach MA, Weber T, Takano E, Breitling R. 2011. antiSMASH: rapid identification, annotation and analysis of secondary metabolite biosynthesis gene clusters in bacterial and fungal genome sequences. Nucleic Acids Res. 39:W339–W346. https://doi.org/10.1093/nar/gkr466

103. Blin K, Shaw S, Augustijn HE, Reitz ZL, Biermann F, Alanjary M, Fetter A,Terlouw BR, Metcalf WW, Helfrich EJN, van Wezel GP, Medema MH, Weber T. 2023. antiSMASH 7.0: New and improved predictions for detection, regulation, chemical structures and visualisation. Nucleic Acids Res. 51:W46–W50. https://doi.org/10.1093/nar/gkad344

104. Alcock BP, Huynh W, Chalil R, Smith KW, Raphenya AR, Wlodarski MA, et al. CARD 2023: expanded curation, support for machine learning, and resistome prediction at the Comprehensive Antibiotic Resistance Database. Nucleic Acids Res. 2023;51: D690–D699. https://doi.org/10.1093/nar/gkac920

105. Mandal S, Bhattacharya S, Roy C, Rameez MJ, Sarkar J, Mapder T, Fernandes S, Peketi A, Mazumdar A, Ghosh W. 2020. Cryptic roles of tetrathionate in the sulfur cycle of marine sediments: microbial drivers and indicators. Biogeosciences 17:4611-4631. https://doi.org/10.5194/bg-17-4611-2020

106. Li D, Liu CM, Luo R, Sadakane K, Lam TW. 2015. MEGAHIT: an ultra-fast single-node solution for large and complex metagenomics assembly via succinct de Bruijn graph. Bioinformatics 31:1674–1676. https://doi.org/10.1093/bioinformatics/btv033

107. Hyatt D, Chen GL, LoCascio PF, Land ML, Larimer FW, Hauser LJ. 2010. Prodigal: prokaryotic gene recognition and translation initiation site identification. BMC Bioinformatics 11:119. https://doi.org/10.1186/1471-2105-11-119

108. Langmead B, Salzberg SL. 2012. Fast gapped-read alignment with Bowtie 2. Nat Methods 9:357–359. https://doi.org/10.1038/nmeth.1923

109. Li H, Handsaker B, Wysoker A, Fennell T, Ruan J, Homer N, Marth G, Abecasis G, Durbin R. 2009. The sequence alignment/map format and SAMtools. Bioinformatics 25:2078-2079. https://doi.org/10.1093/bioinformatics/btp352

LEGENDS

Fig. 1. Geographical location of the Tso Moriri lake, topography of the explored area, and position of the sampling sites. (**a**) Map of northern India showing the location of the Tso Moriri lake. (**b**) Satellite view of the lake shown in the context of the adjoining areas of the Changthang desert (position of the study area is indicated by a yellow square). (**c**) Satellite view of the west bank of Tso Moriri where the study sites (indicated by cyan arrows) were situated. (**d**) Panoramic view of the portion of the lake and the adjoining hill from where samples were collected. (**e**) The barren hill slope where weathered rock dust (fine talus and scree) was sampled for the upper 1 cm from the surface. (**f**) Shallow coastal water of Tso Moriri that was sampled from within a depth of 1 cm. (**g**) Shallow coastal sediment of Tso Moriri that were sampled for the top 1 cm. Maps and views shown in panels (**a**), (**b**) and (**c**) were sourced from the open database located at https://www.google.co.in/maps.

Fig. 2. Growth, survival, or abolition of cell populations documented for the TMA isolates in LB medium under cold or frigid conditions. Growth, or the lack of it, was tested at (**a** and **b**) -10°C, (**c** and **d**) 4°C, or (**e** and **f**) 15°C, and expressed as the increase or decrease in CFU density recorded over time (final CFU count mL^{-1} of the culture as a percentage of the initial value). Every number plotted is an arithmetic mean of the data acquired from three different experiments, where standard deviation always remained <2% of the mean. Numerical values of the CFU densities underlying the data shown in panels (**a** and **b**), (**c** and **d**), and (**e** and **f**) can be found in Tables S1, S2, and S3 respectively. (**g**) Percentage of the initial CFU density retained post incubation by each isolate lacking growth at -10°C is tabulated alongside the percentage of cells remaining metabolically active (capable of taking FDA stain) within the same culture. Refer to Fig. S1 for the flow cytometry-derived dot plots depicting what proportions of cells were stained by FDA in the 14 different isolates incapable of growing at -10°C.

Fig. 3. Abilities of the 27 TMA isolates to grow at near-zero and sub-zero degree Celsius temperatures in MS solution supplemented with one simple or complex carbon compound at a time: **Ac**, acetate; **Ag**, agar; **Al**, albumin; **Bz**, benzoate; **Cl**, cellulose; **Ct**, chitin; **Hd**, hexadecane; **Pt**, pectin; **St**, starch; **Xy**, xylan. After incubation for (**a**) 14 days at 4°C, or (**b**) 28 days at -10°C, growth was considered to have occurred due to the utilization of a given carbon compound only when a positive remainder value was obtained after subtracting the percentage increase in CFU density recorded for the same organism in MS (here also, only positive values were considered) from the percentage increase in CFU density recorded in MS supplemented with the carbon compound in question (here too, only positive values were considered). Numerical values for the percentage increases in CFU-density that were attributable to the utilization of the different carbon compounds at 4°C and -10°C have been given in Tables S14 and S25, while all CFU density values underlying the data shown in Tables S14 and S25 have been presented in Tables S4-S13 and S15-S24, respectively.

Fig.4. Growth, survival, or abolition of cell populations documented for the TMA isolates in LB medium at temperatures above the psychrophilic range. Growth, or the lack of it, was tested at (**a** and **b**) 28°C, (**c** and **d**) 37°C, or (**e** and **f**) 42°C, and expressed as the increase or decrease in CFU density recorded over time (final CFU count mL^{-1} of the culture as a percentage of the initial value). Every number plotted is an arithmetic mean of the data acquired from three different experiments, where standard deviation always remained <2% of the mean. Numerical values of the CFU densities underlying the data shown in panels (**a** and **b**), (**c** and **d**), and (**e** and **f**) can be found in Tables S28, S29, and S30 respectively. (**g**, **h**, and **i**) Percentages of the initial CFU densities retained post incubation by each isolate lacking growth at 28°C, 37°C, and 42°C respectively are tabulated alongside the percentages of cells remaining metabolically active (capable of taking FDA stain) within the same cultures. Refer to Figs. S3a, S3b, and S4 for the flow cytometry-derived dot plots depicting what proportions of cells were stained by FDA in the 4, 16, and 27 different isolates incapable of growing at 28°C, 37°C, and 42°C respectively.

Fig.5. Growth rates (percentages of the initial CFU densities that increased per day of incubation), or absence of growth (no increase in the CFU density over time), recorded for the individual TMA isolates in Luria broth at -10°C, 4°C, 15°C, 28°C, 37°C, and 42°C. Within a given

panel, a green bar indicates an increase recorded in the CFU density over time (growth). Blue bar indicates no increase in CFU density over time, but >1% cells of the culture getting stained with FDA at the end of the incubation. Red bar indicates no increase in CFU density over time, and <1% cells of the culture getting stained with FDA at the end of the incubation. Numerical values for all the CFU densities underlying these graphical representations can be found in Tables S31-S36. FACS data for the proportions of FDA-stained cells can be found in Figs. S1, S3 and S4.

Fig. 6. Graphic representation of growth, survival, or abolition of cell population for different TMA isolates after incubation in Luria broth for 28, 14, 2, 4, 2, and 1 days, at -10°C, 4°C, 15°C, 28°C, 37°C, and 42°C, respectively. (**a**) TMA isolates clustered based on the patterns of their responses to different incubation temperatures in terms of growth, survival, or abolition of cell population. (**b**) TMA isolates clustered on the basis of their isolation source.

Fig. 7. Graphic representation of the antibiosis potentials of the 27 bacterial species isolated from the Tso Moriri area. Green cells indicate growth, while red cells indicate inhibition of growth, for the target organisms.

Fig. 8. Metabolic-category-wise numeral distribution of genes putatively concerned with adaptations to low and high temperatures, within the genomes of the selected TMA isolates. Deep blue bars of the histograms indicate the numbers of genes associated with low temperature adaptation; orange bars indicate the numbers of genes associated with adaptation to low as well as high temperatures. Strains isolated from weathered rock dust, lake-water, and lake-sediment are clustered in boxes shaded grey, cyan, and light orange, respectively. Below each isolate name, a box panel indicating the organism's growth/survival phenotype at the six incubation temperatures tested has been given (the fill color code of the boxes is given at the upper left corner of the figure).

Fig. 9. TMA-isolate-wise numeral distribution of genes putatively concerned with (**a**) all forms of extreme temperature adaptation, (**b**) low temperature adaptation, and (**c**) tandem adaptation to low and high temperatures (central tendencies of the data, post clustering of the strains according to their isolation sources, have been shown). Each isolation-source-specific boxplot displays the mean value (indicated by "+" sign), median value, interquartile range, and minimum–

maximum whiskers, determined for the gene counts (indicated by hollow circles) of the isolates concerned.

Fig. 10. Functional-category-wise numeral distribution of genes putatively concerned with carbohydrate metabolism, within the genomes of the selected TMA isolates. (**a**) Representation of the data in the form of histograms, where grey colored bars indicate the numbers of genes encoding the different categories of carbohydrate-active enzymes (CAZymes). Strains isolated from weathered rock dust, lake-water, and lake-sediment are clustered in boxes shaded grey, cyan, and light orange, respectively. Below each isolate name, a box panel indicating the organism's ability to grow using different carbon compounds (at 4°C and/or -10°C) has been given (the fill color code of the boxes is given below the figure). **(b)** Heatmap representing the functional-category-wise distribution of CAZyme-coding genes in the different TMA isolates (one-way hierarchical clustering of the isolates has also been rendered).

Fig. 11. Schematic diagram showing how indigenous psychrophilic bacteria might render homeostatic control of *in situ* temperature in the context of climate warming and consequential threat of invasion by foreign microbes from warmer territories.

Table 1. Chemoorganoheterotrophic bacteria isolated from three different environments (habitats) within the Tso Moriri area (TMA), viz. lake-water, lake-sediment, and weathered rock dust of a lake-side hill.

Phylum-level affiliation of the isolate(s)	Name of the isolate	Isolation source	Number of sibling strains isolated from the different TMA habitats			Closest bacterial species in the LPSN* (16S rRNA gene sequence similarity in %)	Contigs (length in bp) incorporating the sequenced genome
			Weathered rock dust	Lake-water	Lake-sediment		
Actinomycetota (formerly Actinobacteria)	*Arthrobacter* sp. TRD_SC_1	Weathered rock dust	1	0	0	*Arthrobacter oryzae* KV-651^T (98.84) *Arthrobacter pascens* DSM 20545^T (98.47)	-
	Arthrobacter sp. TRD_SC_3	Weathered rock dust	2	0	0	*Arthrobacter cheniae* Hz2^T (99.64) *Arthrobacter bussei* KR32^T (99.56)	-
	Arthrobacter sp. TRD_SC_4	Weathered rock dust	1	0	0	*Arthrobacter ruber* MDB1-42^T (98.38) *Arthrobacter bussei* KR32^T (98.30)	-
	Arthrobacter sp. TRD_SC_6	Weathered rock dust	1	0	0	*Arthrobacter tumbae* LMG 19501^T (99.22) *Arthrobacter parietis* LMG 22281^T (99.15)	1 circular chromosome (3568629)
	Arthrobacter sp. TRD_SC_8	Weathered rock dust	1	0	0	*Arthrobacter citreus* DSM 20133^T (99.28) *Arthrobacter sunyaminii* zg-ZUI122^T (98.99)	-
	Cryobacterium sp. TS_SC_7	Lake-sediment	0	0	1	*Cryobacterium breve* TMT4-23 (99.14) *Cryobacterium psychrotolerans* 0549 (98.55)	1 circular chromosome (3330347)
	Microbacterium sp. TRD_SC_10	Weathered rock dust	2	0	0	*Microbacterium paraoxydans* CF36 (99.06) *Microbacterium algeriense* G1 (98.84)	-
	Microbacterium sp. TW_SC_2	Lake-water	0	1	0	*Microbacterium algeriense* G1 (99.63) *Microbacterium oxydans* DSM 20578 (99.56)	1 circular chromosome (3289799)
	Microbacterium sp. TW_SC_3	Lake-water	0	1	0	*Microbacterium lacus* A5E-52 (99.05) *Microbacterium invictum* DC-200 (98.83)	-
	Mycetocola sp. TRD_SC_2	Weathered rock dust	5	0	0	*Mycetocola manganoxydans* MB1-14^T (99.48) *Mycetocola miduiensis* MD-T1-10-2^T (99.47)	1 circular chromosome (3111394)
	Paenarthrobacter sp. TRD_SC_7	Weathered rock dust	6	0	0	*Paenarthrobacter nitroguajacolicus* G2-1 (99.18) *Paenarthrobacter aurescens* DSM 20116 (98.81)	1 circular chromosome (4661226)
	Pseudarthrobacter sp. TRD_SC_9	Weathered rock dust	1	0	0	*Pseudarthrobacter psychrotolerans* YJ56 (98.60) *Pseudarthrobacter phenanthrenivorans* Sphe3 (98.1)	1 circular chromosome (3927882)
	Pseudarthrobacter sp. TS_SC_4	Lake-sediment	0	0	2	*Pseudarthrobacter psychrotolerans* YJ56 (99.13) *Pseudarthrobacter siccitolerans* 4J27 (99.06)	-
	Sanguibacter sp. TS_SC_8	Lake-sediment	0	0	1	*Sanguibacter gelidistatuariae* ISLP-3 (99.06) *Sanguibacter suarezii* ST26 (98.70)	1 circular chromosome (4103235)
	Streptomyces sp. TRD_SC_5	Weathered rock dust	2	0	0	*Streptomyces anulatus* NBRC 13369 (98.04) *Streptomyces pratensis* ch24 (98.04)	2 linear large-contigs (7020184 and 364836) 1 circular plasmid (56726)
Bacillota (formerly Firmicutes)	*Trichococcus* sp. TS_SC_9	Lake-sediment	0	0	1	*Trichococcus paludicola* B7-2 (99.72) *Trichococcus pasteurii* KoTa2 (99.72)	1 circular chromosome (3099620)
Bacteroidota (formerly Bacteroidetes)	*Flavobacterium* sp. TS_SC_2	Lake-sediment	0	0	2	*Flavobacterium psychrolimnae* NBRC 102679 (99.63) *Flavobacterium petrolei* Kopri-42 (99.20)	-
	Flavobacterium sp. TS_SC_5	Lake-sediment	0	0	2	*Flavobacterium caseinilyticum* AT-3-2 (99.27) *Flavobacterium psychrolimnae* NBRC 102679 (98.98)	1 circular chromosome (3888044)
Pseudomonadota (class Alphaproteobacteria)	*Ancylobacter* sp. TW_SC_1	Lake-water	0	2	0	*Ancylobacter aquaticus* NBRC 102453 (98.37) *Ancylobacter novellus* DSM 506 (98.37)	1 linear large-contig (4836346) 1 circular plasmid (43214)
Pseudomonadota (class Gammaproteobacteria)	*Acinetobacter* sp. TW_SC_4	Lake-water	0	1	0	*Acinetobacter variabilis* NIPH 2171 (99.43) *Acinetobacter refrigeratoris* WB1 (99.28)	1 circular chromosome (3177979) 2 circular plasmids (181413 and 81896)
	Aeromonas sp. TS_SC_11	Lake-sediment	0	0	10	*Aeromonas salmonicida* CECT 894 (100)	1 linear large-contig (4790999) 2 circular plasmids (89024 and 72486)
	Pseudomonas sp. TS_SC_1	Lake-sediment	0	0	1	*Pseudomonas mandelii* NBRC 103147 (99.86) *Pseudomonas silesiensis* A3 (99.86)	-
	Pseudomonas sp. TS_SC_3	Lake-sediment	0	0	1	*Pseudomonas guineae* M8 (99.78) *Pseudomonas leptonychotis* CCM 8849 (99.57)	1 circular chromosome (4036479)
	Pseudomonas sp. TS_SC_10	Lake-sediment	0	0	2	*Pseudomonas crudilactis* UCMA 17988 (98.92) *Pseudomonas helmanticensis* OHA11 (98.70)	-
	Pseudomonas sp. TS_SC_12	Lake-sediment	0	0	3	*Pseudomonas cuatrocienegasensis* 1N (99.56) *Pseudomonas borbori* R-20821 (98.62)	-
	Pseudomonas sp. TS_SC_13	Lake-sediment	0	0	1	*Pseudomonas cannabina* CFBP 2341 (98.50) *Pseudomonas congelans* P 538/23 (98.50)	-
	Psychrobacter sp. TS_SC_6	Lake-sediment	0	0	7	*Psychrobacter cryohalolentis* K5 (99.78) *Psychrobacter glaciei* BIc20019 (99.21)	1 circular chromosome (2931123) 3 circular plasmids (23102, 7109 and 6426)

* List of Prokaryotic names with Standing in Nomenclature (88).

Table 2. Genomic potentials of the TMA isolates for the synthesis of, and resistance against, different classes of antibiotic and secondary metabolite.

Isolation source	Name of the isolate	Antibiotics potentially synthesized	Secondary metabolites synthesized	Antibiotics potentially resisted
Weathered rock dust	*Arthrobacter* sp. TRD_SC_6	-	NAPAAs[1], NI-siderophores[2]	-
	Mycetocola sp. TRD_SC_2	-	NAPAAs, Type-III polyketides	-
	Paenarthrobacter sp. TRD_SC_7	Penicillins and cephalosporins	NAPAAs, NI-siderophores, NRPs[3]	Rifamycins
	Pseudarthrobacter sp. TRD_SC_9	Staurosporines	NAPAAs, NI-siderophores, Type-III polyketides	-
	Streptomyces sp. TRD_SC_5	Staurosporines, Vancomycins	Class-II Lanthipeptides, Class-III Lanthipeptides, NI-siderophores, NRPs, Terpenes, Type-I polyketides	Rifamycins
Lake - water	*Acinetobacter* sp. TW_SC_4	-	-	-
	Ancylobacter sp. TW_SC_1	-	NRPs, Type-I polyketides	-
	Microbacterium sp. TW_SC_2	-	Type-III polyketides	-
Lake-sediment	*Aeromonas* sp. TS_SC_11	-	NRPs, NRP-metallophores[4], Terpenes	Carbapenems, Cephalosporins, Elfamycins, Penicillin and other beta-lactams
	Cryobacterium sp. TS_SC_7	Prodigiosin	NAPAAs, Terpenes, Type-III polyketides	-
	Flavobacterium sp. TS_SC_5	-	Terpenes	-
	Pseudomonas sp. TS_SC_3	-	-	Diaminopyrimidines, Fluoroquinolones, Phenicols
	Psychrobacter sp. TS_SC_6	-	-	-
	Sanguibacter sp. TS_SC_8	Tetracyclines	NAPAAs	Rifamycins
	Trichococcus sp. TS_SC_9	-	Type-III polyketides	-

[1] NAPAAs: non-alpha poly-amino acids
[2] NI-siderophores: siderophores independent of non-ribosomal peptide synthase
[3] NRPs: non-ribosomal peptides
[4] NRP-metallophores: non-ribosomal peptide (NRP) metallophores

a
National Park
Боги миллии
Bokhtar
Курғонтеппа
Hotan
Prefecture
Skardu
LADAKH
Kabul
Peshawar
Srinagar
JAMMU AND
KASHMIR
Leh
0
200.41 km
Tso Moriri
Jammu
Sargodha
HIMACHAL
PRADESH
Lahore
Jalandhar
CHANDIGARH
Multan
PUNJAB
UTTARAKHAND
Pakistan
Bahawalpur
HARYANA
New Delhi
Rahim
Yar Khan
Nepal
Sukkur
UTTAR
PRADESH
b
Karzok
Karzok
Tso Moriri
Manechan
Google Earth
c
d
e
f
g

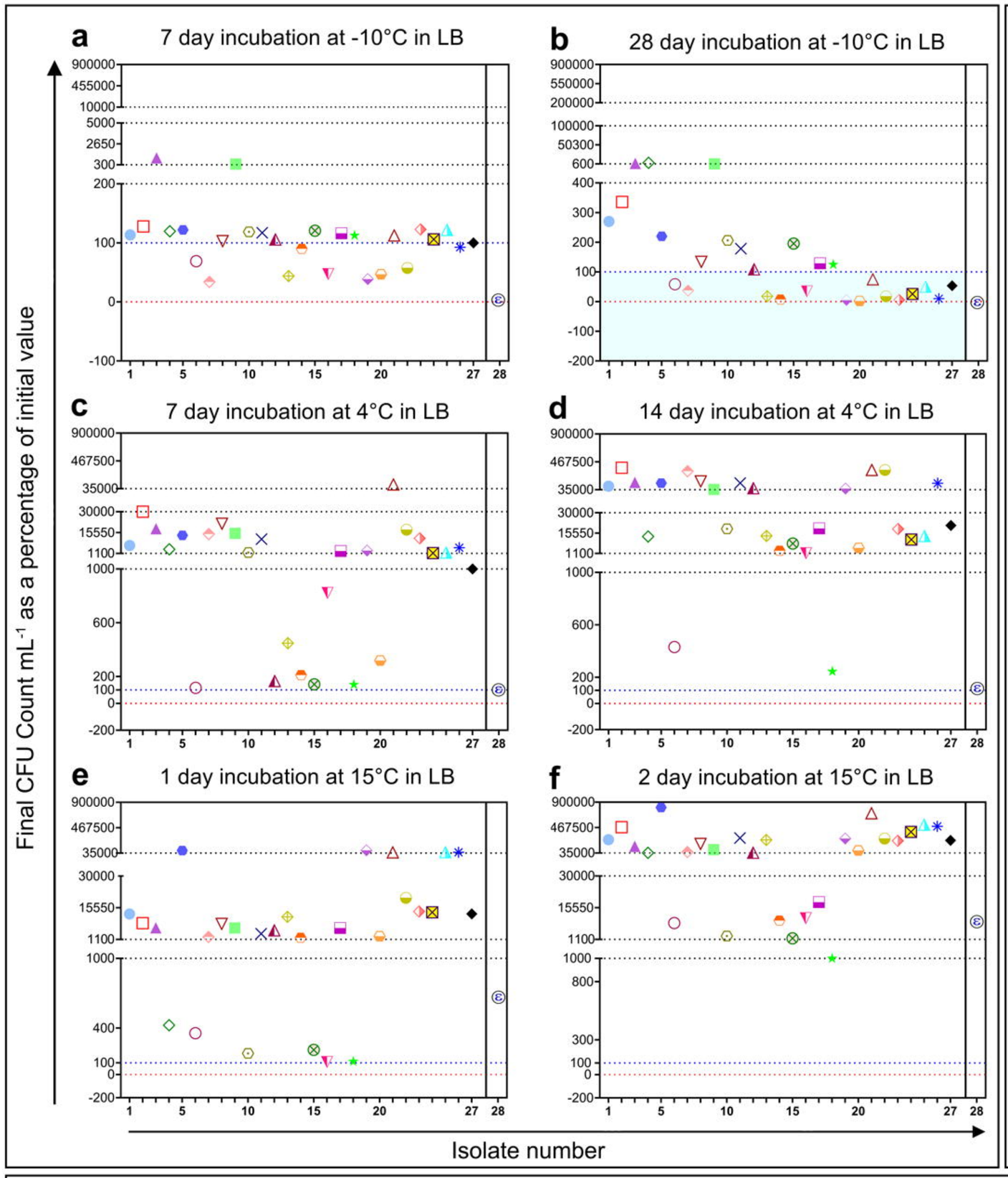

g Phenotypes of the strains lacking growth at -10°C

Strain name	Percentage of CFUs retained after 28 days at -10°C	Percentage of cells remaining metabolically active after 28 days at -10°C
Cryobacterium sp. TS_SC_7	58.5	99.3
Microbacterium sp. TRD_SC_10	37.1	95.8
Pseudarthrobacter sp. TS_SC_4	17.8	18.8
Sanguibacter sp. TS_SC_8	7	99.2
Ancylobacter sp. TW_SC_1	34.7	87.2
Flavobacterium sp. TS_SC_5	4.9	93.1
Acinetobacter sp. TW_SC__4	2	75.7
Aeromonas sp. TS_SC_11	75	95.5
Pseudomonas sp. TS_SC_1	17.4	87.7
Pseudomonas sp. TS_SC_3	5.7	35.1
Pseudomonas sp. TS_SC_10	25.5	46.8
Pseudomonas sp. TS_SC_12	50	67
Pseudomonas sp. TS_SC_13	10	81.7
Psychrobacter sp. TS_SC_6	53.5	90

1) *Arthrobacter* sp. TRD_SC_1
2) *Arthrobacter* sp. TRD_SC_3
3) *Arthrobacter* sp. TRD_SC_4
4) *Arthrobacter* sp. TRD_SC_6
5) *Arthrobacter* sp. TRD_SC_8
6) *Cryobacterium* sp. TS_SC_7
7) *Microbacterium* sp. TRD_SC_10
8) *Microbacterium* sp. TW_SC_2
9) *Microbacterium* sp. TW_SC_3
10) *Mycetocola* sp. TRD_SC_2
11) *Paenarthrobacter* sp. TRD_SC_7
12) *Pseudarthrobacter* sp. TRD_SC_9
13) *Pseudarthrobacter* sp. TS_SC_4
14) *Sanguibacter* sp. TS_SC_8
15) *Streptomyces* sp. TRD_SC_5
16) *Ancylobacter* sp. TW_SC_1
17) *Trichococcus* sp. TS_SC_9
18) *Flavobacterium* sp. TS_SC_2
19) *Flavobacterium* sp. TS_SC_5
20) *Acinetobacter* sp. TW_SC_4
21) *Aeromonas* sp. TS_SC_11
22) *Pseudomonas* sp. TS_SC_1
23) *Pseudomonas* sp. TS_SC_3
24) *Pseudomonas* sp. TS_SC_10
25) *Pseudomonas* sp. TS_SC_12
26) *Pseudomonas* sp. TS_SC_13
27) *Psychrobacter* sp. TS_SC_6
28) *Escherichia coli* K-12

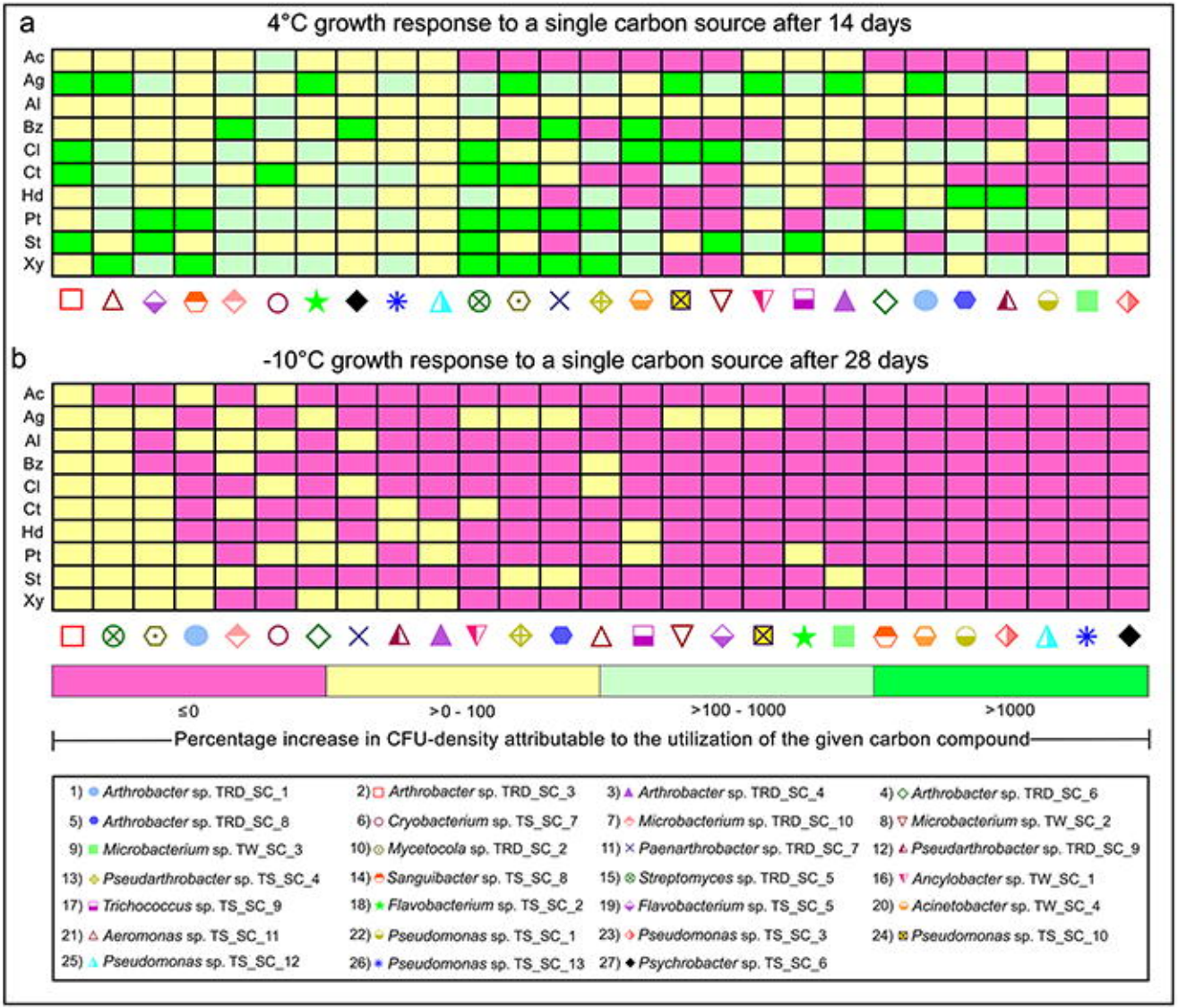
a
4°C growth response to a single carbon source after 14 days
Ac
Ag
Al
Bz
Cl
Ct
Hd
Pt
St
Xy
b
-10°C growth response to a single carbon source after 28 days
Ac
Ag
Al
Bz
Cl
Ct
Hd
Pt
St
Xy
≤0
>0 - 100
>100 - 1000
>1000
Percentage increase in CFU-density attributable to the utilization of the given carbon compound
1) Arthrobacter sp. TRD_SC_1
2) Arthrobacter sp. TRD_SC_3
3) Arthrobacter sp. TRD_SC_4
4) Arthrobacter sp. TRD_SC_6
5) Arthrobacter sp. TRD_SC_8
6) Cryobacterium sp. TS_SC_7
7) Microbacterium sp. TRD_SC_10
8) Microbacterium sp. TW_SC_2
9) Microbacterium sp. TW_SC_3
10) Mycetocola sp. TRD_SC_2
11) Paenarthrobacter sp. TRD_SC_7
12) Pseudarthrobacter sp. TRD_SC_9
13) Pseudarthrobacter sp. TS_SC_4
14) Sanguibacter sp. TS_SC_8
15) Streptomyces sp. TRD_SC_5
16) Ancylobacter sp. TW_SC_1
17) Trichococcus sp. TS_SC_9
18) Flavobacterium sp. TS_SC_2
19) Flavobacterium sp. TS_SC_5
20) Acinetobacter sp. TW_SC_4
21) Aeromonas sp. TS_SC_11
22) Pseudomonas sp. TS_SC_1
23) Pseudomonas sp. TS_SC_3
24) Pseudomonas sp. TS_SC_10
25) Pseudomonas sp. TS_SC_12
26) Pseudomonas sp. TS_SC_13
27) Psychrobacter sp. TS_SC_6

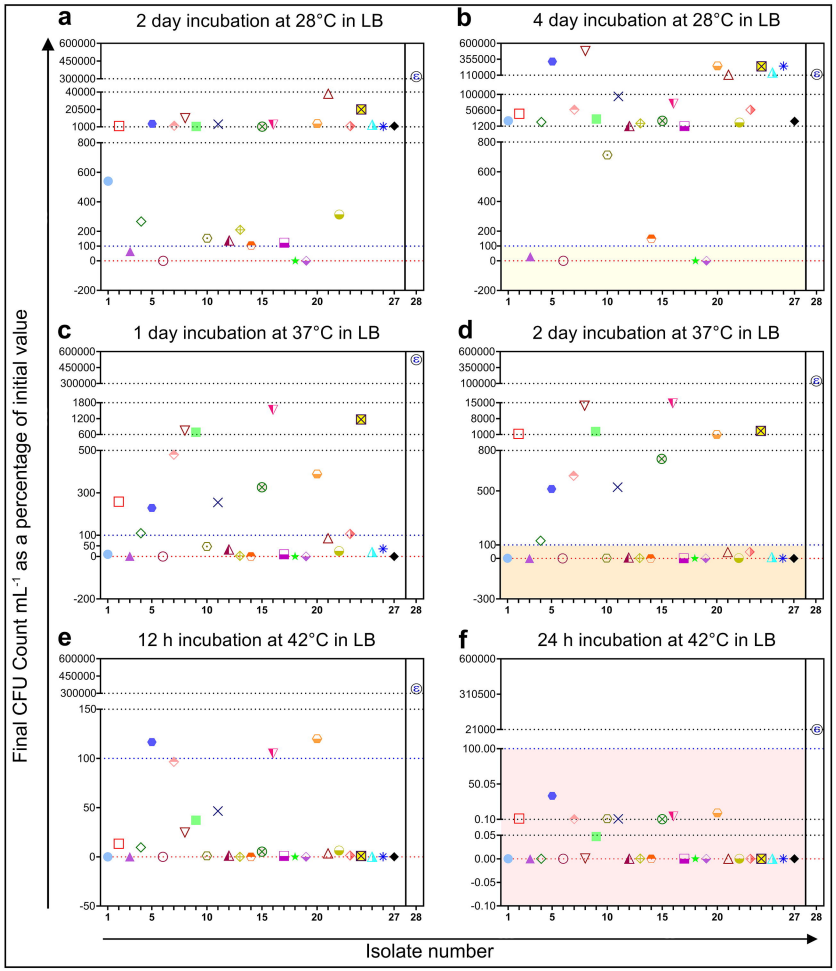

Phenotypes of the strains lacking growth at 28°C, 37°C and/or 42°C

g

Strain name	Percentage of CFUs retained after four days at 28°C	Percentage of cells remaining metabolically active after four days at 28°C
Arthrobacter sp. TRD_SC_4	27.6	58.4
Cryobacterium sp. TS_SC_7	0	0.2
Flavobacterium sp. TS_SC_2	0	18.2
Flavobacterium sp. TS_SC_5	0	21.6

h

Strain name	Percentage of CFUs retained after two days at 37°C	Percentage of cells remaining metabolically active after two days at 37°C
Arthrobacter sp. TRD_SC_1	0.8	20.1
Arthrobacter sp. TRD_SC_4	0.04	10.5
Cryobacterium sp. TS_SC_7	0	0.1
Mycetocola sp. TRD_SC_2	2.4	45
Pseudarthrobacter sp. TRD_SC_9	6.1	47.7
Pseudarthrobacter sp. TS_SC_4	2.2	4.5
Sanguibacter sp. TS_SC_8	0.04	4.2
Trichococcus sp. TS_SC_9	0.4	7.5
Flavobacterium sp. TS_SC_2	0	4
Flavobacterium sp. TS_SC_5	0	10.4
Aeromonas sp. TS_SC_11	46.4	65.1
Pseudomonas sp. TS_SC_1	1.7	39.7
Pseudomonas sp. TS_SC_3	48.2	58.8
Pseudomonas sp. TS_SC_12	8.9	19.7
Pseudomonas sp. TS_SC_13	0.4	75.9
Psychrobacter sp. TS_SC_6	0.01	39.3

i

Strain name	Percentage of CFUs retained after one day at 42°C	Percentage of cells remaining metabolically active after one day at 42°C
Arthrobacter sp. TRD_SC_1	0	15
Arthrobacter sp. TRD_SC_3	1.2	7.2
Arthrobacter sp. TRD_SC_4	0	0.1
Arthrobacter sp. TRD_SC_6	0	0.1
Arthrobacter sp. TRD_SC_8	33.3	39.9
Cryobacterium sp. TS_SC_7	0	0
Microbacterium sp. TRD_SC_10	0.4	14.7
Microbacterium sp. TW_SC_2	0.001	57.9
Microbacterium sp. TW_SC_3	0.1	58.1
Mycetocola sp. TRD_SC_2	1.1	43.4
Paenarthrobacter sp. TRD_SC_7	0.8	18.4
Pseudarthrobacter sp. TRD_SC_9	0	45.5
Pseudarthrobacter sp. TS_SC_4	0.0004	0.9
Sanguibacter sp. TS_SC_8	0	1.1
Streptomyces sp. TRD_SC_5	0.4	10.9
Ancylobacter sp. TW_SC_1	4.3	49.4
Trichococcus sp. TS_SC_9	0	0.03
Flavobacterium sp. TS_SC_2	0	0.2
Flavobacterium sp. TS_SC_5	0	0.1
Acinetobacter sp. TW_SC_4	9.3	87.3
Aeromonas sp. TS_SC_11	0	57.4
Pseudomonas sp. TS_SC_1	0	31.4
Pseudomonas sp. TS_SC_3	0	0.1
Pseudomonas sp. TS_SC_10	0	5.9
Pseudomonas sp. TS_SC_12	0	15
Pseudomonas sp. TS_SC_13	0	41.2
Psychrobacter sp. TS_SC_6	0	12.7

1) *Arthrobacter* sp. TRD_SC_1
2) *Arthrobacter* sp. TRD_SC_3
3) *Arthrobacter* sp. TRD_SC_4
4) *Arthrobacter* sp. TRD_SC_6
5) *Arthrobacter* sp. TRD_SC_8
6) *Cryobacterium* sp. TS_SC_7
7) *Microbacterium* sp. TRD_SC_10
8) *Microbacterium* sp. TW_SC_2
9) *Microbacterium* sp. TW_SC_3
10) *Mycetocola* sp. TRD_SC_2
11) *Paenarthrobacter* sp. TRD_SC_7
12) *Pseudarthrobacter* sp. TRD_SC_9
13) *Pseudarthrobacter* sp. TS_SC_4
14) *Sanguibacter* sp. TS_SC_8
15) *Streptomyces* sp. TRD_SC_5
16) *Ancylobacter* sp. TW_SC_1
17) *Trichococcus* sp. TS_SC_9
18) *Flavobacterium* sp. TS_SC_2
19) *Flavobacterium* sp. TS_SC_5
20) *Acinetobacter* sp. TW_SC_4
21) *Aeromonas* sp. TS_SC_11
22) *Pseudomonas* sp. TS_SC_1
23) *Pseudomonas* sp. TS_SC_3
24) *Pseudomonas* sp. TS_SC_10
25) *Pseudomonas* sp. TS_SC_12
26) *Pseudomonas* sp. TS_SC_13
27) *Psychrobacter* sp. TS_SC_6
28) *Escherichia coli* K-12

Temperature windows for population-level growth/survival of the TMA isolates

Increase recorded in CFU density over time (growth percentage value plotted along Y axis)

No increase in CFU density over time, but >1% cells metabolically-active post incubation

No increase in CFU density over time, and <1% cells metabolically-active post incubation

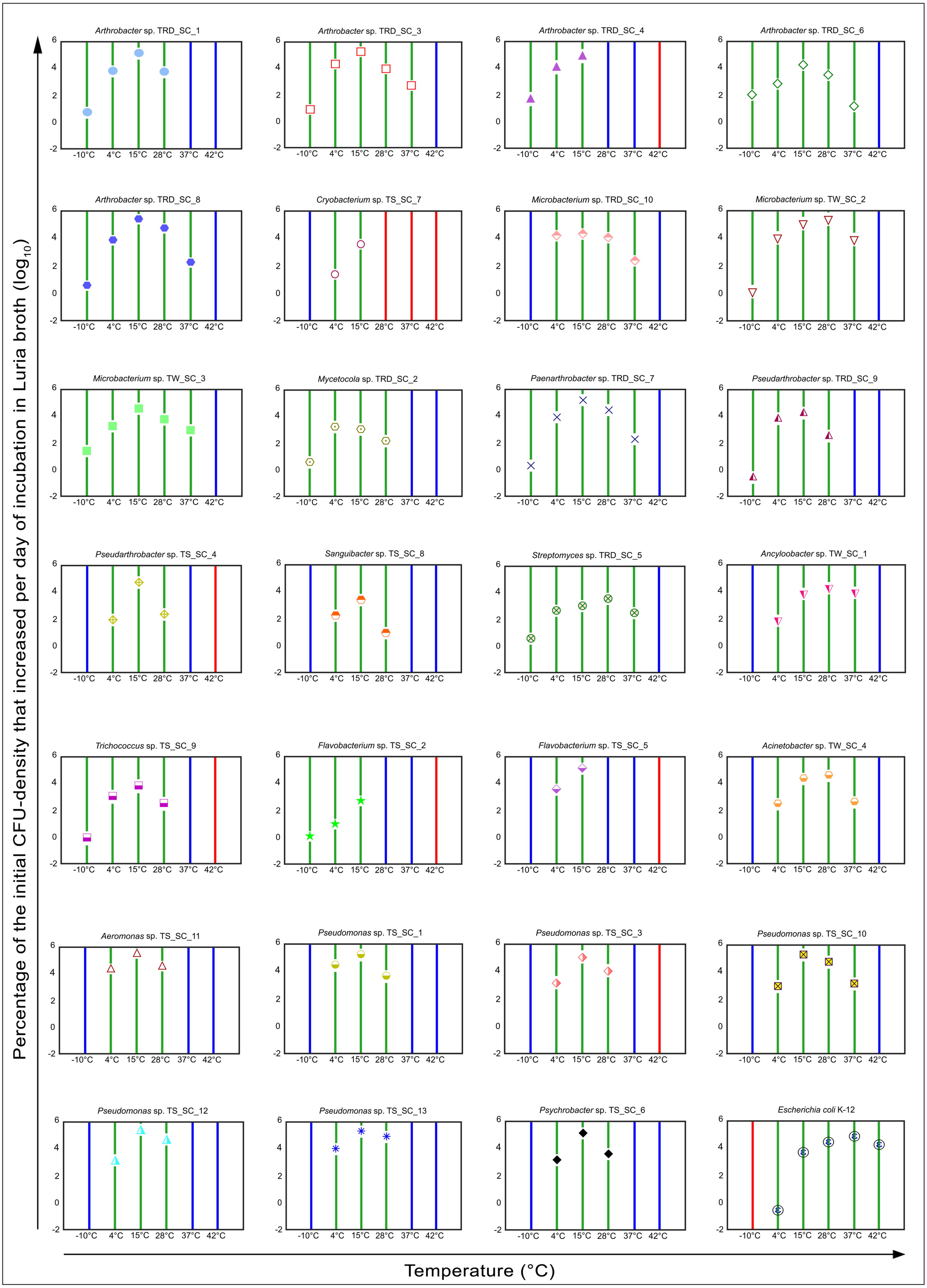

a

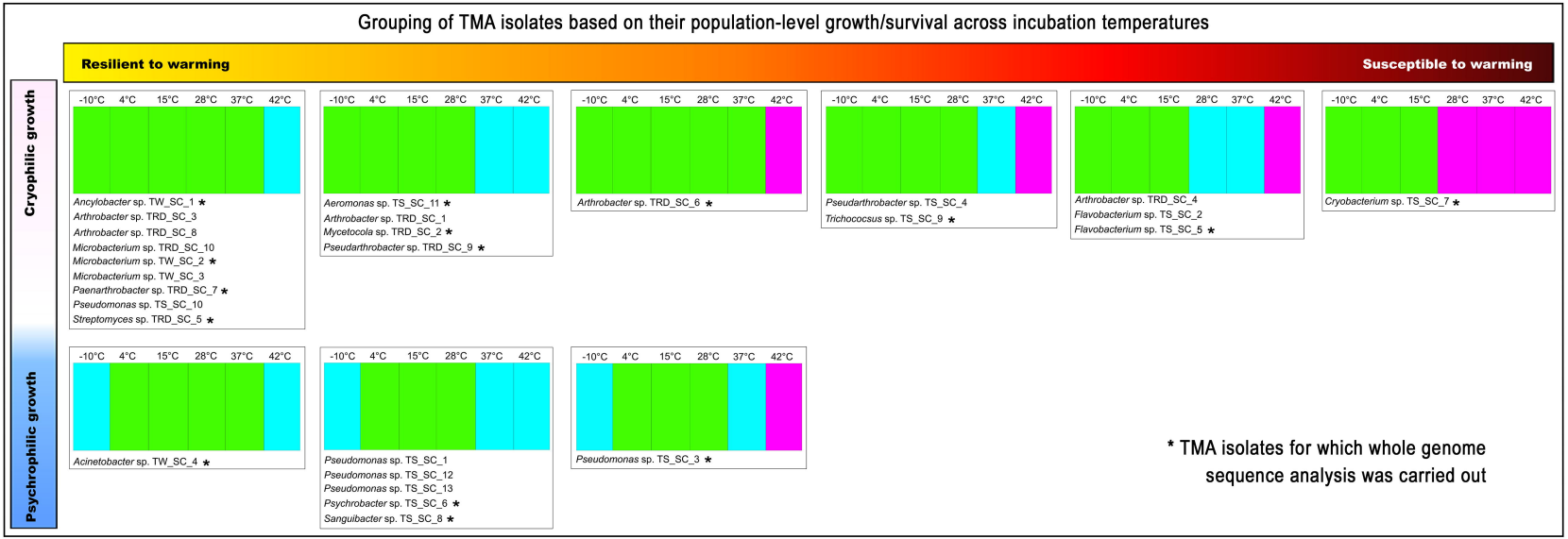

b

Incubation-temperature-dependent growth/survival of the TMA species grouped based on their isolation sources

Weathered rock dust of lake side hill						
Strain	Temperature (°C)					
	-10	4	15	28	37	42
Arthrobacter sp. TRD_SC_3						
Arthrobacter sp. TRD_SC_8						
Paenarthrobacter sp. TRD_SC_7						
Streptomyces sp. TRD_SC_5						
Microbacterium sp. TRD_SC_10						
Arthrobacter sp. TRD_SC_1						
Mycetocola sp. TRD_SC_2						
Pseudarthrobacter sp. TRD_SC_9						
Arthrobacter sp. TRD_SC_6						
Arthrobacter sp. TRD_SC_4						

Lake water						
Strain	Temperature (°C)					
	-10	4	15	28	37	42
Microbacterium sp. TW_SC_2						
Microbacterium sp. TW_SC_3						
Ancylobacter sp. TW_SC_1						
Acinetobacter sp. TW_SC_4						

Lake sediment						
Strain	Temperature (°C)					
	-10	4	15	28	37	42
Pseudomonas sp. TS_SC_10						
Aeromonas sp. TS_SC_11						
Pseudomonas sp. TS_SC_1						
Pseudomonas sp. TS_SC_12						
Pseudomonas sp. TS_SC_13						
Psychrobacter sp. TS_SC_6						
Sanguibacter sp. TS_SC_8						
Trichococcus sp. TS_SC_9						
Pseudarthrobacter sp. TS_SC_4						
Pseudomonas sp. TS_SC_3						
Flavobacterium sp. TS_SC_2						
Flavobacterium sp. TS_SC_5						
Cryobacterium sp. TS_SC_7						

Increase recorded in the CFU densities of LB, and/or single C-compound, grown cultures

No increase in CFU density in any type of medium, but >1% cells of the LB culture stained with FDA

No increase in CFU density in any type of medium, and <1% cells of the LB culture stained with FDA

Isolates tested as targets of antibiosis (spread in the form of liquid incolum on LA plates already dotted with antagonist colonies)

Isolates tested as antagonists of growth of other bacteria (pre-established as colonies on LA plates)

Origin and identity of the organisms tested			Actinobacteria															Non-Actinobacteria
			Isolates from the weathered rock dust of a lake-side hill										Isolates from lake-water		Isolates from lake-sediment			Isolates from lake-water and lake-sediment
			Arthrobacter TRD_SC_1	*Arthrobacter* TRD_SC_3	*Arthrobacter* TRD_SC_4	*Arthrobacter* TRD_SC_6	*Arthrobacter* TRD_SC_8	*Microbacterium* TRD_SC_10	*Mycetocola* TRD_SC_2	*Paenarthrobacter* TRD_SC_7	*Pseudarthrobacter* TRD_SC_9	*Streptomyces* TRD_SC_5	*Microbacterium* TW_SC_2	*Microbacterium* TW_SC_3	*Cryobacterium* TS_SC_7	*Pseudarthrobacter* TS_SC_4	*Sanguibacter* TS_SC_8	The 12 different species were tested individually
Mesophiles from other habitats	Gram positive bacteria	*Lysinibacillus fusiformis* LAPE1_SD1																
		Bacillus licheniformis PAMA2_SD1																
		Bacillus subtilis SC_1																
	Gram negative bacteria	*Advenella kashmirensis* WT001																
		Paracoccus SMMA_5																
		Escherichia coli K-12																
Tso Moriri isolates outside Actinomycetota	Isolates from lake-sediment	*Aeromonas* TS_SC_11																
		Flavobacterium TS_SC_2																
		Flavobacterium TS_SC_5																
		Pseudomonas TS_SC_1																
		Pseudomonas TS_SC_3																
		Pseudomonas TS_SC_10																
		Pseudomonas TS_SC_12																
		Pseudomonas TS_SC_13																
		Psychrobacter TS_SC_6																
		Trichococcus TS_SC_9																
	Isolates from lake-water	*Acinetobacter* TW_SC_4																
		Ancylobacter TW_SC_1																
Tso Moriri isolates belonging to Actinomycetota	Isolates from lake-sediment	*Sanguibacter* TS_SC_8																
		Pseudarthrobacter TS_SC_4																
		Cryobacterium TS_SC_7																
	Isolates from lake-water	*Microbacterium* TW_SC_3																
		Microbacterium TW_SC_2																
	Isolates from the weathered rock dust of a lake-side hill	*Streptomyces* TRD_SC_5																
		Pseudarthrobacter TRD_SC_9																
		Paenarthrobacter TRD_SC_7																
		Mycetocola TRD_SC_2																
		Microbacterium TRD_SC_10																
		Arthrobacter TRD_SC_8																
		Arthrobacter TRD_SC_6																
		Arthrobacter TRD_SC_4																
		Arthrobacter TRD_SC_3																
		Arthrobacter TRD_SC_1																

Uninhibited lawn of growth observed for the incoming organism, around the pre-established colony of the antagonist

Clear zone of inhibition observed for the incoming organism, around the pre-established colony of the antagonist.

Increase recorded in the CFU densities of LB and/ or single C-compound grown cultures
No increase in CFU density in any type of medium,but >1% cells of the LB culture took FDA stain
No increase in CFU density in any type of medium, and <1% cells of the LB culture took FDA stain
Number of genes present in the genome for
Low temperature adaptation
Adaptation to both low and high temperatures
Cold-shock protein synthesis / RNA remodeling
Membrane fluidity regulation
Genome maintenance
Chaperone synthesis / protein quality control
DNA repair / oxidative stress management
Global gene regulation
Compatible solute / osmoprotectant metabolism
1 16
1 15
1 3
1 16
1 18
1 31
1 33
Weathered rock dust isolates
Streptomyces TRD_SC_5
Paenarthrobacter TRD_SC_7
Pseudarthrobacter TRD_SC_9
Arthrobacter TRD_SC_6
Mycetocola TRD_SC_2
Lake-water isolates
Ancylobacter TW_SC_1
Microbacterium TW_SC_2
Acinetobacter TW_SC_4
Lake-sediment isolates
Aeromonas TS_SC_11
Pseudomonas TS_SC_3
Trichococcus TS_SC_9
Flavobacterium TS_SC_5
Sanguibacter TS_SC_8
Cryobacterium TS_SC_7
Psychrobacter TS_SC_6
Incubation temperatures (°C)
-10 4 15 28 37 42

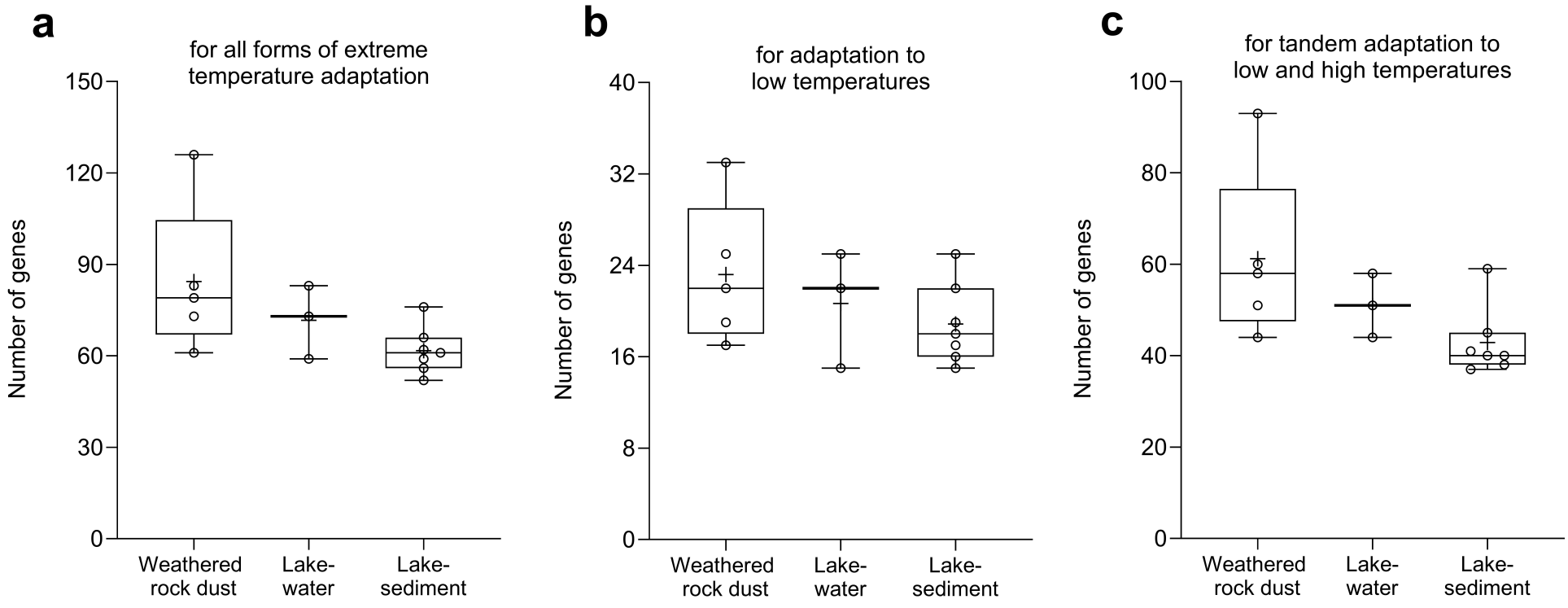
a
for all forms of extreme temperature adaptation
Number of genes
150
120
90
60
30
0
Weathered rock dust
Lake-water
Lake-sediment
b
for adaptation to low temperatures
Number of genes
40
32
24
16
8
0
Weathered rock dust
Lake-water
Lake-sediment
c
for tandem adaptation to low and high temperatures
Number of genes
100
80
60
40
20
0
Weathered rock dust
Lake-water
Lake-sediment

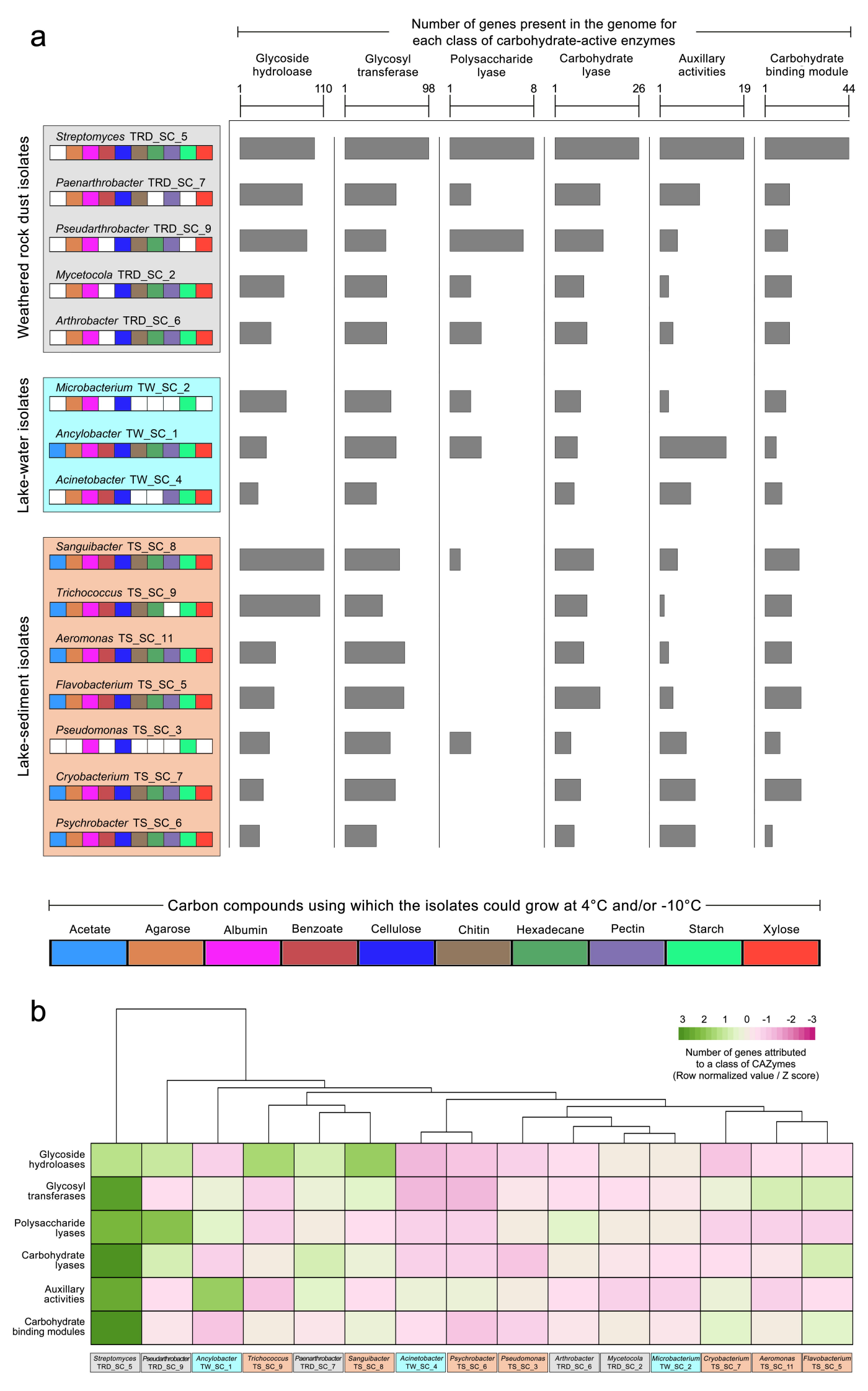
a
Number of genes present in the genome for each class of carbohydrate-active enzymes
Glycoside hydroloase
1
110
Glycosyl transferase
1
98
Polysaccharide lyase
1
8
Carbohydrate lyase
1
26
Auxillary activities
1
19
Carbohydrate binding module
1
44
Weathered rock dust isolates
Streptomyces TRD_SC_5
Paenarthrobacter TRD_SC_7
Pseudarthrobacter TRD_SC_9
Mycetocola TRD_SC_2
Arthrobacter TRD_SC_6
Lake-water isolates
Microbacterium TW_SC_2
Ancylobacter TW_SC_1
Acinetobacter TW_SC_4
Lake-sediment isolates
Sanguibacter TS_SC_8
Trichococcus TS_SC_9
Aeromonas TS_SC_11
Flavobacterium TS_SC_5
Pseudomonas TS_SC_3
Cryobacterium TS_SC_7
Psychrobacter TS_SC_6
Carbon compounds using wihich the isolates could grow at 4°C and/or -10°C
Acetate
Agarose
Albumin
Benzoate
Cellulose
Chitin
Hexadecane
Pectin
Starch
Xylose
b
3 2 1 0 -1 -2 -3
Number of genes attributed to a class of CAZymes (Row normalized value / Z score)
Glycoside hydroloases
Glycosyl transferases
Polysaccharide lyases
Carbohydrate lyases
Auxillary activities
Carbohydrate binding modules
Streptomyces TRD_SC_5
Pseudarthrobacter TRD_SC_9
Ancylobacter TW_SC_1
Trichococcus TS_SC_9
Paenarthrobacter TRD_SC_7
Sanguibacter TS_SC_8
Acinetobacter TW_SC_4
Psychrobacter TS_SC_6
Pseudomonas TS_SC_3
Arthrobacter TRD_SC_6
Mycetocola TRD_SC_2
Microbacterium TW_SC_2
Cryobacterium TS_SC_7
Aeromonas TS_SC_11
Flavobacterium TS_SC_5

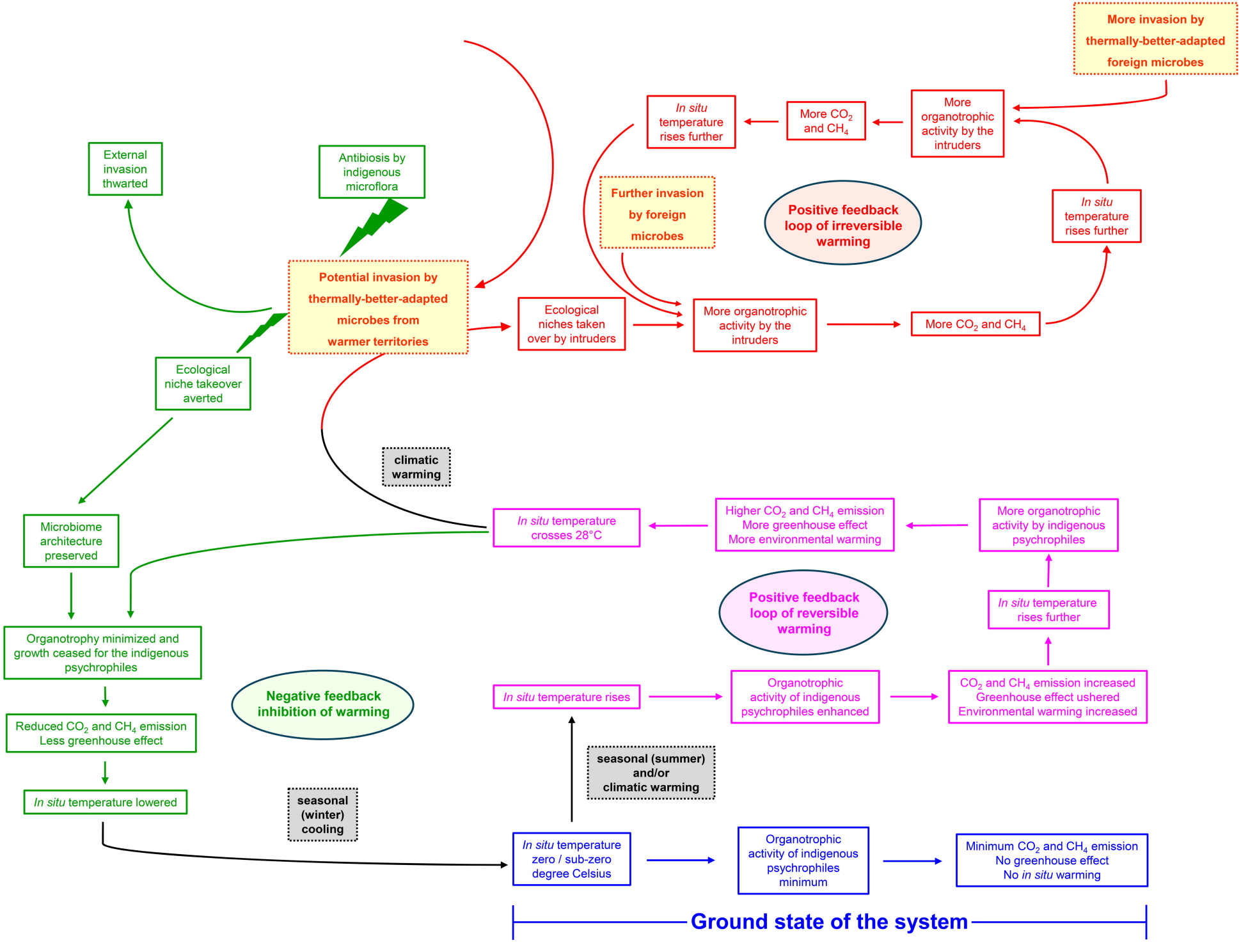
More invasion by thermally-better-adapted foreign microbes
In situ temperature rises further
More CO_2 and CH_4
More organotrophic activity by the intruders
External invasion thwarted
Antibiosis by indigenous microflora
Further invasion by foreign microbes
Positive feedback loop of irreversible warming
In situ temperature rises further
Potential invasion by thermally-better-adapted microbes from warmer territories
Ecological niches taken over by intruders
More organotrophic activity by the intruders
More CO_2 and CH_4
Ecological niche takeover averted
climatic warming
Microbiome architecture preserved
In situ temperature crosses 28°C
Higher CO_2 and CH_4 emission
More greenhouse effect
More environmental warming
More organotrophic activity by indigenous psychrophiles
Positive feedback loop of reversible warming
In situ temperature rises further
Organotrophy minimized and growth ceased for the indigenous psychrophiles
Negative feedback inhibition of warming
In situ temperature rises
Organotrophic activity of indigenous psychrophiles enhanced
CO_2 and CH_4 emission increased
Greenhouse effect ushered
Environmental warming increased
Reduced CO_2 and CH_4 emission
Less greenhouse effect
seasonal (summer) and/or climatic warming
In situ temperature lowered
seasonal (winter) cooling
In situ temperature zero / sub-zero degree Celsius
Organotrophic activity of indigenous psychrophiles minimum
Minimum CO_2 and CH_4 emission
No greenhouse effect
No in situ warming
Ground state of the system